Biomechanical Analyses of Head Acceleration during Contact Sports

and Ankle Joint Complex Injury

By

Bardiya Akhbari

Submitted to the graduate degree program in Mechanical Engineering and the Graduate Faculty of the University of Kansas in partial fulfillment of the requirements for the degree of Master of Science.

_____

Chairperson Dr. Lorin P. Maletsky

_____

Dr. Sara E. Wilson

_____

Dr. Carl W. Luchies

Date Defended: July 22nd, 2016

The Thesis Committee for Bardiya Akhbari

certifies that this is the approved version of the following thesis:

Biomechanical Analyses of Head Acceleration during Contact Sports

and Ankle Joint Complex Injury

_____

Chairperson Dr. Lorin P. Maletsky

Date approved: July 27th, 2016

Abstract

Athletes are frequently exposed to conditions that can result in bodily injuries, such as concussions and ankle sprains. This research is divided into two separate biomechanical studies: the design and evaluation of a device to simulate football helmet collisions and its parameters, and a cadaveric study to investigate the effects of ankle sprains.

An impactor system was designed and built along with a computational model to simulate football helmet collisions, test helmet designs, and evaluate the influence of different parameters on head acceleration. Peak head accelerations of 20g to 60g, and rise times were targeted based on measures reported in the literature. A computational model of the impactor system was developed in Adams to determine design parameters such as neck stiffness and dampening. A pendulum impactor was constructed to achieve various impact energies by changing the release angle of the arm reaching up to 110 J. A dummy's neck was designed as a single degree-of-freedom hinge joint with variable stiffness. Peak head accelerations agreed within 6% of literature reported accelerations. Similar to previous studies, the head reaches its peak acceleration in 10 to 12 ms. Neck stiffness did not affect the head peak acceleration during the 20 ms following impact. Moreover, the computational model revealed that adding a dampening of 1.75 N.s/mm to the neck results in 20 g decrease in the head peak acceleration.

A second study aimed both to characterize the effects of collateral ankle ligament injuries using nine cadaveric ankle joints and to quantify the contribution of lower leg muscle forces to the ankle joint kinematics. Intact ankles were tested, then anterior talofibular (ATFL) and calcaneofibular (CFL) ligaments were sequentially resected to simulate two grades of ankle injury. The tibialis anterior (TA) and extensor digitorum longus (EDL) tendons were loaded with static weights and distributed based on their physiological cross sectional area. Weak TA and Weak EDL

configuration were simulated by reducing their respective muscle loads by 50%. The ankle was moved from full dorsiflexion to plantarflexion using a stepper motor attached to Achilles tendon. The effect of muscle configuration (Weak TA and Weak EDL) and injuries (ΔATFL and ΔATFL-CFL) compared to baseline (intact ankle with physiological load set) on the measured ankle joint kinematics was determined using a repeated measures ANOVA. The weaker EDL demonstrated 1° to 3° higher inversion than physiological loads through the cycle significantly. After the simulated ATFL-CFL injury, the trials demonstrated a 2° increase in inversion with respect to intact ankle kinematics in dorsiflexion. The required Achilles' load increased by up to 24% in plantarflexion after the injury indicating a significant reduction in efficiency. Based on the higher inversion results in weaker muscle set, strengthening the EDL might help to prevent the hyper inversion injuries.

Acknowledgements

This work would not have been possible without the guidance and assistance of several people who have helped me throughout my graduate study at KU and I owe a special thanks to them. I dedicate this work to them.

First and foremost to my family: my father, mother and brother for their support, encouragement and believing in me. Without their love and support none of this would have been possible.

To my advisor, Prof. Lorin Maletsky for giving me this opportunity. I have learned a lot from him as a researcher and as a person. He really pushed and encouraged me to be my best and without him I would not be the engineer I am today. I never forget Outlier or Salt Lake. Thanks for believeing in me.

To Prof. Luchies who taught me to use Adams software effectively, and supervised me to be a better tutor and teacher assistant. To Prof. Wilson who taught me the ethics in the engineering.

To all the faculty members and staff of the Mechanical engineering departments, especially Dr. Surana, Dr. Fang, Dr. K, Kate, Jim, and Stephanie for their time and effort.

To Fallon G. Fitzwater. An awesome colleague who helped me a lot through the helmet study. Without her advice and help this was not possible. Thanks for everything. Thanks for being my friend though I made you crazy here and there.

To Sami Shalhoub. A remarkable colleague who helped me a lot through the helmet and the ankle study. Thanks for believeing in me. A friend who educated and helped me in coding and everything. So many long days and weeks that we worked on the KKS. Thanks, Thanks, Thanks!

To Matthew Hastings Dickinson. A wonderful colleague, who helped me a lot in the ankle study. We started working as newbies and I believe that we are not newbies anymore. To those days that

we did not have any clue what are we doing. To the day that we started testing ankles at 4AM and finished at midnight. So many great memories. Thanks.

To Charles Gabel and Ash Shadrick for their advice and patience in the machine shop.

To Uncle Masoud, Aunt Maryam, Donna, and Donniel: Without your care, the life was harder here. Having you near me and in my thought was one of the best thing that I have had here. Knowing that I have a family that are like my parents was a blessing.

To all my friends who were awesome in the past two years: Masih, Payam, Rouzbeh, Mobin, Armita, Shima, Nazanin, Salma, Masoud, Ali, PK, Parisa, Behnaz, Nick, Niki, Eileen, Hadley, Ednah, Lance and many others. You made my life easier and gave me the energy to keep up.

List of Abbreviations

ATFL	Anterior Talofibular Ligament
CFL	Calcaneofibular Ligament
PTFL	Posterior Talofibular Ligament
TA	Tibialis Anterior
EDL	Extensor Digitorum Longus
PCSA	Physiological Cross Sectional Area
AnPo	Anterior Posterior
InEv	Inversion Eversion
IntExt	Internal External
AJC	Ankle Joint Complex
mTBI	Mild Traumatic Brain Injuries
cTBI	Chronic Traumatic Brain Injuries
NOCSAE	National Operating Committee on Standards for Athletic Equipment
NFL	National Football League
LI	Linear Impactors

List of Figures

List of Tables

Table of Contents

1. Introduction

One of the nation's most popular sport, American football, is a full-contact sport with tackles and severe impact collisions as a regular part of the game. Given its full-contact nature, American football players are at a high risk for injuries, namely concussion and ankle injuries. Observing a high rate of injuries per athlete-exposures, this research is focused on both subjects and tried to improve understanding of the injuries with the goal of preventing them or enhancing the rehabilitation. Among the injuries, ankle injuries are one of the most common injuries in all sports, and head concussion is the most common injury in all contact sports (Payne et al., 1997; Thurman et al., 1998). While many studies reported on these topics, there are still factors, such as muscle contribution in the ankle injury and the influence of neck stiffness on the head acceleration after collisions, which need to be assessed. This current work is divided into two separate biomechanical studies. The first study developed a system to evaluate concussion-level helmet impacts. The second study utilized cadaveric ankle specimens to investigate ankle sprains.

Sports-related brain injuries happen with an estimated range of 1.6 to 3.8 million cases every year only in the Unites States. Almost 300,000 of these injuries are concussions that occur while playing contact sports, especially football with the largest number of incidences. Most commonly, a concussion is caused by severe impact to the helmet or other part of the body such as the shoulder pad or even the knee. These harsh collisions transmit a large force from the helmet to the head, which results in a large translational head acceleration, possibly leading to a concussion. Helmets have been designed to reduce peak head acceleration and have led to a reduction of concussion rates to some degree (Bartsch et al., 2012b); however, they can be improved and there are numerous objectives that could be tested to improve our understanding of the collision and its impacts. By designing and validating a pendulum impactor system that can

simulate helmet-helmet collisions experienced by football players, the impact can be replicated. Subsequently, other parameters' influence on the head acceleration, such as neck stiffness, can be evaluated.

Furthermore, injuries to the ankle joint are one of the most common sports injuries. Inversion injuries account for 80% of ankle's injuries result in the rupture or sprain of the collateral ligaments and can lead to joint instability (Brooks et al., 1981; Brostroem, 1964; Slimmon and Brukner, 2010). While the ligaments could be repaired or replaced in surgery, changes in the muscle activity have been seen after the injuries and their subsequent rehabilitation. Thus, the main muscles of the foot will be activated differently after the joint rehabilitation. Understanding the effects of collateral ligaments during the injury as well as the effect of muscle contribution might be helpful for designing rehabilitation sessions or simplifying the diagnosis procedure. Moreover, quantifying the effects of the muscle contribution on the ankle joint complex will aid in muscle function analysis after injury by determining the effects of muscles weakness on the ankle joint kinematics.

The current research has two seperate objectives: 1) design a machine for simulating the helmet collisions and evaluate the influence of neck stiffness on the head and helmet acceleration after the impact, and 2) characterize the collateral ligament injuries in an *in-vitro* model of the ankle joint and analyze the muscle contribution to it. The results of the first study will give a better understanding of helmet and neck contributions to reducing the head acceleration. Moreover, with a machine that can replicate football collisions, it is feasible to test new helmet designs and parameters which could influence the reduction of head acceleration in the future. The results of the second study will give a better understanding of the influence of different muscle loading configurations on the ankle joint kinematics and a profounder understanding of the injury.

2. Helmet Testing Devices and Methods

In the Unites States, sports-related brain injuries occur with an estimated range of 1.6 to 3.8 million cases every year (Crisco and Greenwald, 2011; Gerbeding, 2003; Langlois et al., 2006). Almost 300,000 of these injuries are concussions from playing contact sports, especially football which has the largest number of incidences (Thurman et al., 1998). Generally, a concussion is a form of traumatic brain injury, mostly mild traumatic brain injury (mTBI), caused by severe impacts to the head or to the body. The impact shakes the brain inside the skull and momentarily stops the brain from functioning normally. Impact collisions transmit large forces from the helmet to the head and can lead to a concussion.

2.1. Head Acceleration Measurement

Based on the regulatory standards (NOCSAE, 1998, 2006; Pellman et al., 2006), researchers commonly evaluate concussions by determining the head linear accelerations after the collision. In a well-known study, King et al. revealed that helmets do not change the angular head acceleration significantly, and since the helmets are reducing the concussion rates in the athletes (Bartsch et al., 2012b), thus the linear acceleration should have a greater importance in the head injury assessment (King et al., 2003). Rowson et al. study by introducing a novel technique proposed that studies need to focus on the complex inputs of linear and angular acceleration to evaluate the injury (King et al., 2003; Rowson and Duma, 2013). In another study, Kleiven claimed that even a rotational acceleration is more distinctive for concussion and helmet's assessment, since the linear acceleration decreases equally for different brand helmets (Kleiven, 2013). All in all, it is still not widely agreed whether concussion-level injury is more exclusively related to rotational acceleration or translational acceleration (King et al., 2003).

Combining video analysis and dummy reenactments of impacts from games introduced another method for measuring the head acceleration. Newman (Newman et al., 2000), and Pellman (Pellman et al., 2003a; Pellman et al., 2003b) published a series of papers on concussive impacts that were recorded on film from two or more different angles. Using these video data to reconstruct the angle of the impact, speed of the impact, and the resultant player kinematics, they provided the essential information to recreate the impact conditions with instrumented Hybrid-III dummies in the laboratory. Analyzing 174 impacts, they reported the mean linear head acceleration of 98g for a player receiving a brain injury, and mean linear head acceleration of 60g for cases without a brain injury.

Implementing logistic regression on 53 cases from Newman and Pellman studies, King et al. further quantified the brain kinematics (King et al., 2003). In their regression model, the linear acceleration was considered as the independent variable and the occurrence of an mTBI as the dependent variable. The product of this procedure projected a 25%, 50%, and 75% likelihood of mTBI at a peak linear acceleration of 57.0 g, 79.3 g, and 98.4 g, respectively.

In a more recent study, Rowson et al. analyzed 1712 impacts in collegiate football players and presented resultant linear head acceleration curves with a peak in 10 milliseconds (Rowson et al., 2009). The collisions were for all directions and none of them resulted in a player's concussion. The contact duration of 14 milliseconds was confirmed in their study, as well. In another study, Bartsch et al. compared the new helmet designs and the old leather helmets based on their head acceleration curves (Bartsch et al., 2012b). The authors claimed that the helmets were reducing the head linear acceleration in a same amount, thus the new helmet designs do not reduce the concussion severity, significantly. However, this study considered only a small number of old helmets and only one site of impact location was considered.

2.2. Football Helmet Testing Machines

To assess current and novel helmet designs, machines with an ability to simulate the various impact energies that occur in football collisions have been designed. The simulation consists of certain properties and features which need to be achieved, namely, impact energy level of helmet collisions, the head or helmet peak acceleration, and contact duration. Current guidelines chiefly use three main pass/fail criteria when inspecting a helmet, which are the drop test, linear impacting, and pendulum impacting. All of these machines have the ability to replicate aforementioned factors in the helmet collisions.

The drop test (Figure 2.1) is the main standard procedure for testing the helmets based on National Operating Committee on Standards for Athletic Equipment (NOCSAE) (NOCSAE, 1998). The drop test machine use free fall dynamics which achieves larger impact energy and velocity when the drop height is increased. The rigid surface on the bottom (anvil) and a foam mimics the 10 – 14 millisecond contact duration based on the literature (Pellman et al., 2003b; Pellman et al., 2006; Rowson et al., 2009). While the drop test is very popular because of its simplicity, it has some inherent drawbacks. First, the maximum height limits the maximum achievable velocity of the impact (3.2 m height gives 8 m/sec impact velocity). Moreover, the simulation only considers the mass of the head and helmet in collision and does not consider the torso or body weight. While there are some modified versions of the drop test apparatus (e.g. helmet impactor tower or twin wire drop test) which resolves some of the drawbacks, Hernandez et al. claimed that drop tests are not a suitable experiment for the evaluation of helmets' ability to prevent the mTBI or cTBI (Hernandez et al., 2015). Nevertheless, drop testing is a popular method of checking the helmets to see if they pass the minimum requirements of reducing the head acceleration.

Linear impactors (LI) (Figure 2.2 and Figure 2.3) are designed to simulate a collision with the range of impact velocities from 6 m/s to 12 m/s, which are known to cause mTBI on the playing field (NOCSAE, 2006). The LI includes a pressurized air tank attached to a pneumatic actuator that accelerates the ram. Moreover, the impactor head can freely move after the impact in a guided fashion. The collision is often incomplete during helmet contacts, meaning that the striking player rebounds and moves freely, which the LI is able to simulate while the drop test could not. By adjusting the weight of the impactor head, the striking player's body weight can be imitated to generate more impact energy; however, the struck player was not considered in the machine. Currently, linear impactors are getting more attention because the literature believes that they are superior to drop test for evaluating the response of the helmets for mTBI (Gwin et al., 2010a; Johnston et al., 2015; Pellman et al., 2006).

The pendulum helmet impactors, using the compound pendulum mechanics, are able to simulate different impact energies and velocities by changing the release drop angle (Figure 2.4). Since the pendulum head mass is adjustable, the struck player head velocity can be simulated for better collision replication. The pendulum head and its surface are modified to replicate a contact duration similar to that in helmet collisions (Pellman et al., 2006). Also, the motion of the striking player can be adjusted and evaluated similar to the LI systems. The first pendulum designed by Biokinetics (Ottawa, Ontario, Canada) was scrutinized by National Football League (NFL) committee on mTBI; however, Pellman et al. modified the machine by mounting the dummy on a sled and adjusting the pendulum head weight to achieve better replication of the collisions (Pellman et al., 2006; Withnall and Bayne, 2004).

2.3. Dummy Designs

While NOCSAE suggests specific head weights or filling materials for surrogate head models to be used in football helmet testing, there is not a specific standardized model of the neck-head designs for the surrogates. Currently, the Hybrid III 50th percentile male anthropomorphic test device (Humanetics Innovative Solutions, Plymouth, MI) (Figure 2.5.A), which is the standard human surrogate in crash tests for automotive safety, is getting attention in athletic injury laboratory studies.

The Hybrid III head and neck was built based on the Mertz data (Mertz and Patrick, 1971) to exhibit the same biofidelity or humanlike response. The neck replicated by a deformable body shows different responses in different directions, such as having lower stiffness while rotating to extension than flexion (Spittle et al., 1992). In addition, the neck is capable of large deformations in all directions. Made of viscoelastic materials, comprising butyl rubbers and steel plates, the neck structure closely matches the human neck's nonlinear characteristics (Figure 2.5.B). The butyl rubber replicates the human neck stiffness and damping characteristics and the steel plates provide the correct mass and contribute to the inertial effects during impact. The Hybrid III neck contains a steel cable that runs through its midpoint which indicated the torque to be 12 in-lb; however, this only prevents the rotation of the neck at outsized angles and does not alter the stiffness characteristics of the neck (Figure 2.5.C).

In addition to Hybrid III, there is another neck design like BioRID (Linder et al., 1998), which is designed for rear-end impacts with low speed. Their structure allows neck twist and lateral neck bending. However, since the impacts that are significant in the football field are high speed and energy level collisions, BioRID cannot be used in the laboratory, thus Hybrid III is more common.

Hybrid III was designed and validated for the automotive-type impacts; however, they are not tuned for football collisions. Bartsch et al. evaluated the biofidelity of the neck-head segment of the dummy in various impact locations and stated that the dummy can emulate some of the the impacts; however, Gwin et al. claimed that the neck stiffness should be higher for the football testing, since the players are bracing themselves before most of the impacts (Bartsch et al., 2012a; Gwin et al., 2010b).

The neck stiffness cannot be changed in Hybrid III, which prevents studying of the neck stiffness effects on the head and helmet acceleration curves. In this study, we decided to construct a neck as hinge joint using torsion and extension springs. Having the capability of replacing or adding the springs to increase the stiffness, we were able to evaluate the stiffness effects. Moreover, since the neck design is comprised of modular pieces, the neck can be modified for evaluation of other parameters like dampening or non-linearity in the future studies.

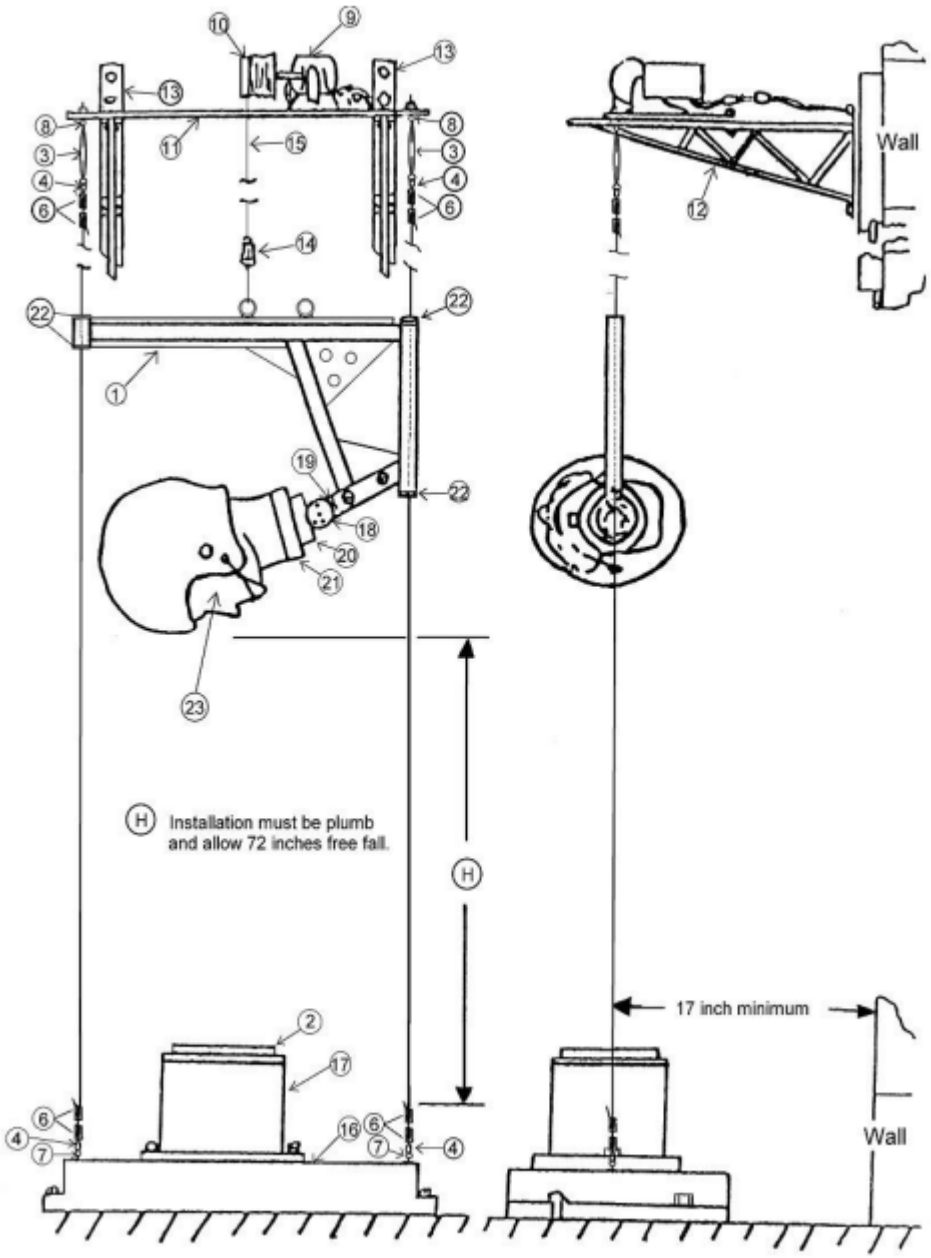

Figure 2.1. Drop test drawing (NOCSAE, 1998)

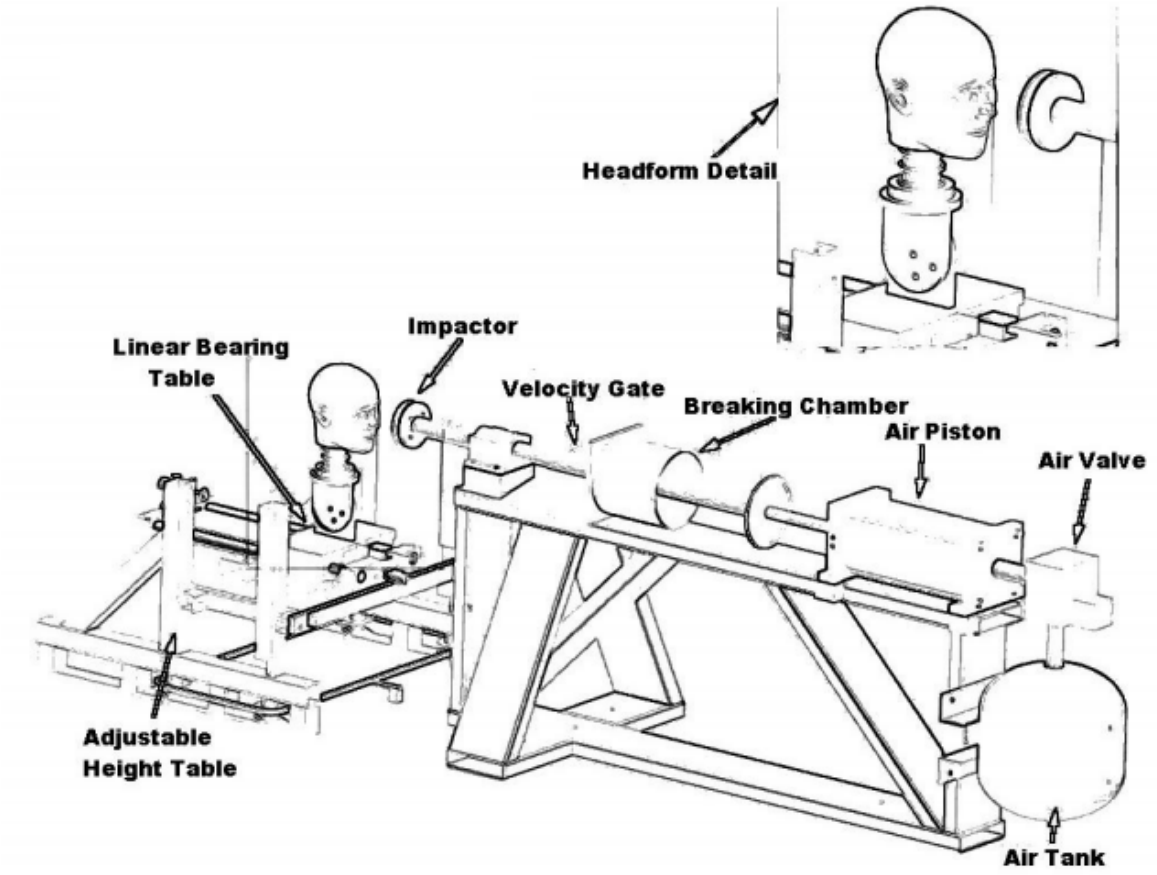

Figure 2.2. Linear impactor drawing (NOCSAE, 2006)

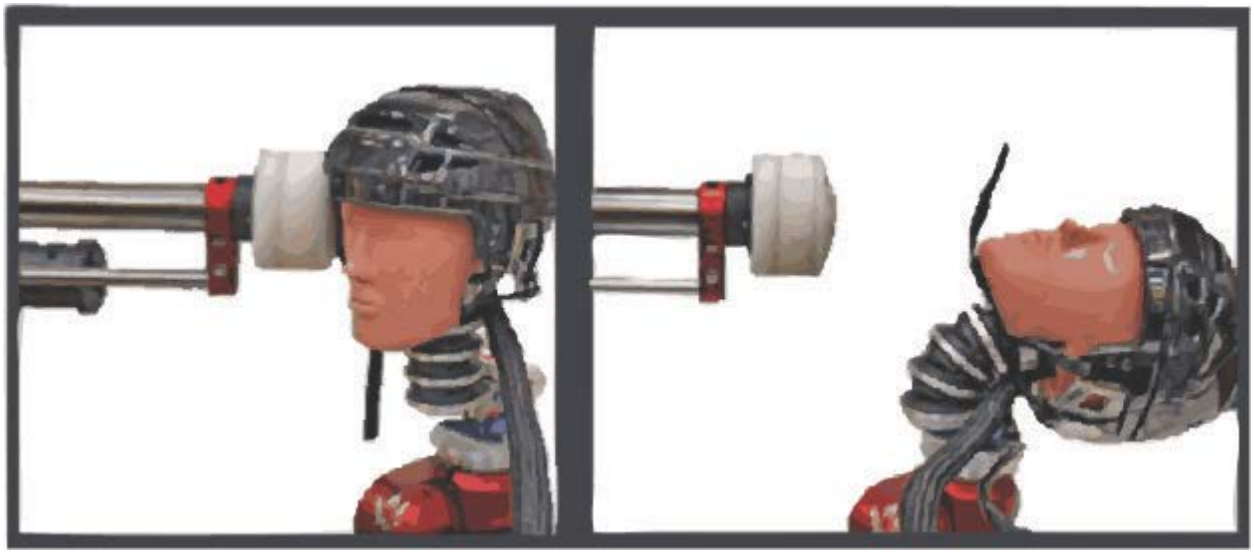

Figure 2.3. Linear impactor in action (TheShockBox, 2016)

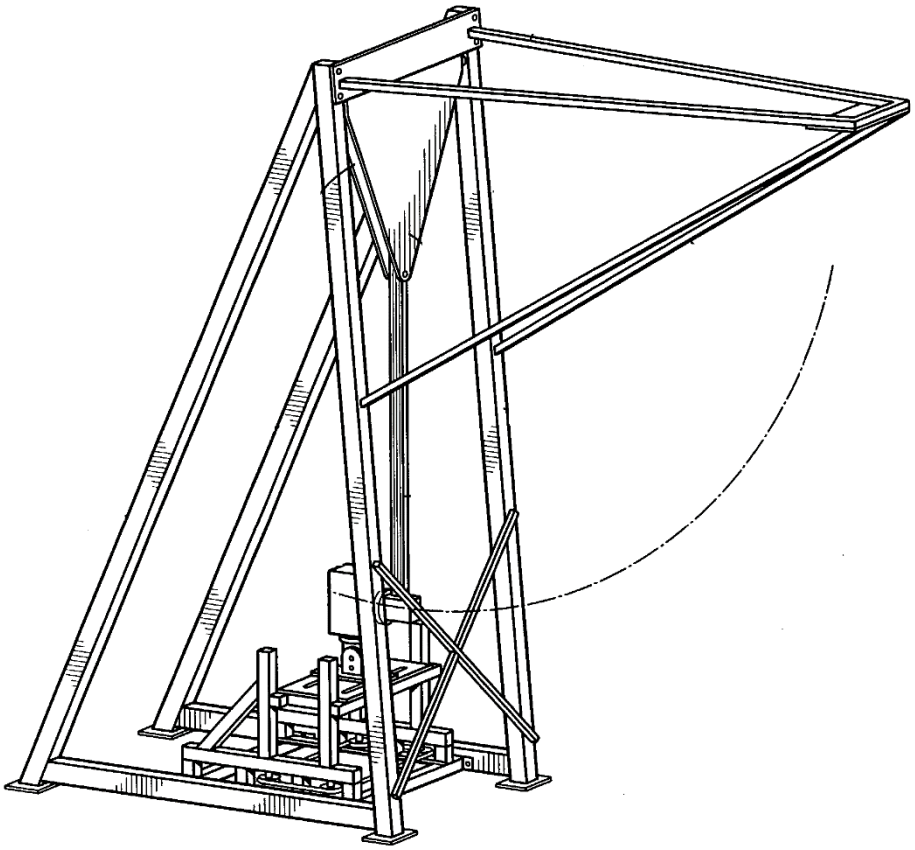

Figure 2.4. Pendulum impactor drawing (Withnall and Bayne, 2004)

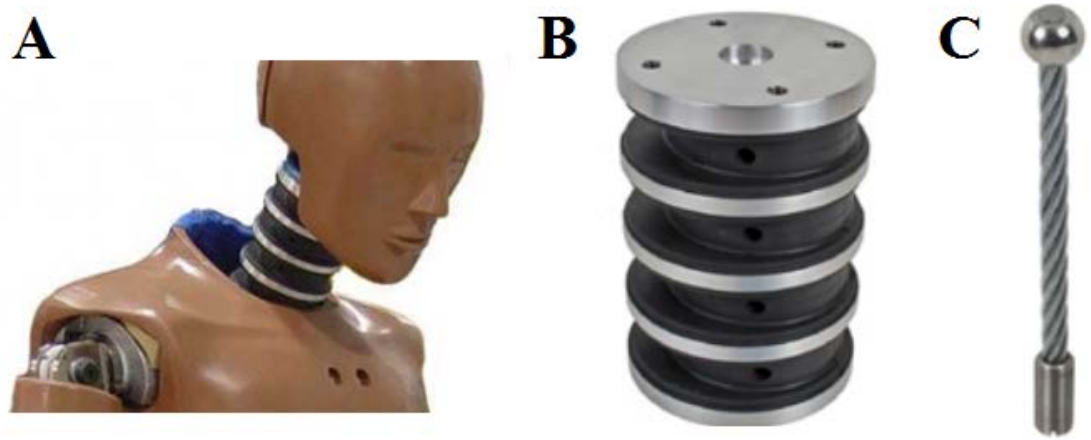

Figure 2.5. Hybrid III dummy. (A) The assembled head and neck parts, (B) Neck molded, comprised of butyl rubbers and steel plates, and (C) neck cable (Humanetics Innovative Solutions, Plymouth, MI)

3. Development of a Machine and Its Computational Model to Evaluate the Influence of Neck Stiffness in Football Collisions

3.1. Introduction

It is estimated that 1.6 to 3.8 million sport-related brain injuries occur in the United States each year (Crisco and Greenwald, 2011; Gerbeding, 2003; Langlois et al., 2006). Almost 300,000 of these brain injuries are concussions, with football having the largest number of incidences (Thurman et al., 1998). Generally, a concussion is a form of mild traumatic brain injury (mTBI), which can subsequently develop into chronic traumatic brain injuries (cTBI). Severe impacts to the helmet or other parts of the body often result in large forces or accelerations in the head. While the purpose of helmet and protective gear is to reduce peak head accelerations and reduce the risk of concussion, they cannot completely prevent it and a peak head acceleration of 80 g will likely lead to a concussion (Bartsch et al., 2012b). Equipment used by the National Football League (NFL) is tested under the guidelines and standards set by the National Operating Committee on Standards for Athletic Equipment (NOCSAE). However, recently, studies have challenged the guideline's proficiency in preventing mTBI and cTBI (Bartsch et al., 2012a; Gwin et al., 2010a; Hernandez et al., 2015).

To assess current and novel helmet designs, a variety of impacting machines have been used to evaluate the impact mechanics experienced by football players during collisions. Current guidelines chiefly use three main pass/fail inspecting machines, which are drop test, linear impacting, and pendulum impacting (NOCSAE, 1998, 2006; Pellman et al., 2003b). These machines have been designed with the ability to simulate various impacts in the laboratory aiming to replicate impact energy, impact velocity, the head and helmet peak accelerations, and contact duration observed in football collisions. While in the drop test the striking player cannot be

emulated, and the hydraulic system of linear impactors is expensive, pendulum impactors are able to simulate different impact energies and velocities simply and inexpensively using compound pendulum mechanics. The mass of the pendulum head can be adjusted to vary the struck player velocity, and the swing height can be varied to change the impact energy levels without any difficulty. Using a computational model further decreases the cost of constructing the machine by evaluating and predicting the dynamics of the motion such as the influence of the neck spring stiffness or line of action in advance.

The Hybrid III 50th percentile male anthropomorphic test device, which is the standard human surrogate in the crash tests for automotive safety, has been used recently in biomechanical analyses of head collisions in football and soccer (Bartsch et al., 2012a; Funk et al., 2009; Lewis et al., 2001; Viano et al., 2012; Withnall and Bayne, 2004). Although the Hybrid III neck torque-load can be changed up to 12 in-lb, some studies stated that the neck stiffness might affect the helmet and head acceleration curves after the collision (Bartsch et al., 2012a; Bartsch et al., 2012b; Funk et al., 2009; Gwin et al., 2010a). Since the stiffness of the neck cannot be changed in the Hybrid III, it would be advantageous to have a head-neck design with the ability to adjust the neck stiffness to determine the effects of neck stiffness on the head accelerations. This new design gives the researcher the ability of simulating various collision conditions like when athletes brace their neck before impact.

The first objective of this study was to design and validate a pendulum impactor system that can simulate collisions experienced by football players. Impact simulations aim to replicate peak helmet accelerations, rise time, contact duration, and impact energies within the range of physiological responses reported in the literature. In order to achieve the first objective, a computational model of the impactor system was used to determine critical design decisions. The

second objective was to use this impactor system to quantify the effects of neck stiffness on helmet dynamics for a variety of impact energies.

3.2. Materials and Methods

3.2.1. Computational Modeling

A three-dimensional computational model was developed for the purpose of predicting the effects of testing machine parameters like frame height and neck factors, such as dampening or spring parameters (Figure 3.1). The model was developed in the computer-aided engineering package MSC.Adams (MSC Software Corporation, Santa Ana, CA) (Appendix A). MSC.Adams formulates and solves the dynamic equations of motion for a given system of constraint that include rigid bodies, forces, torques, joints, springs, dampers, and contacts.

The masses of the head, torso, and the head impactor assemblies were measured directly. The masses for the impactor frame, and arm were calculated using their dimensions and material properties. The moment of inertia for the head was simplified as an ellipsoid. The mass moment of inertia for other parts were calculated based on their CAD geometry, and the computational models were constructed based on those. Also, it was assumed that the sled and rails are travelling freely and without any frictions.

The computational model of the impactor was used to evaluate changing various parameters of the impactor, such as release angle, impactor head weight, impactor arm length, and of the dummy, such as spring stiffness, spring preloads, adding different dampers, and dummy weights (Appendix B). The swing heights (dropping angle) and the pendulum head weight were changed in the computational model to find the impact energy levels of 7, 25.4, and 54.4 Joules based on the literature (Bartsch et al., 2012a). In addition, the computational model was used to determine the effects of extension springs (spring parameters: attachment site, free length,

stiffness, and preload) and dampening mechanism on the peak head acceleration and time to peak acceleration.

3.2.2. The Impactor and Dummy

The impactor, developed at the University of Kansas, is a pendulum impactor with the ability to simulate controlled helmet football collisions. The impactor has the ability to simulate and control three main parameters: impact energy, impact velocity, and contact duration.

The impactor frame is constructed of 80/20 Inc. (Columbia City, Indiana) building material with an overall height of 2.44 m (Figure 3.2). The pendulum pivots about two steel tapered roller bearings. The pendulum arm is constructed of a hollow rectangular tube with a length of 1.52 m. The arm is instrumented with an inclinometer to measure the angular position of the pendulum arm during impact testing at rate of 100 Hz (DOG1 MEMS-Series Inclinometer, Measurement Specialties, Aliso Viejo, CA). The hammer impactor head is made of low carbon steel and has a base weight of 6.8 kg, which can be adjusted to 9.1 kg and 11.3 kg to simulate various impact energy and velocity levels. The effective pendulum mass is 9.0 kg ± 0.5 kg with a minimum of 75% effective mass concentrated in the pendulum head. The pendulum arm can be positioned at a maximum initial position of 90° with a maximum drop height of 1.80 m from the ground or 1.40 m from the helmet.

The dummy system was created using a plastic head and torso from a mannequin (MN-249 Plastic 3/4 Torso Male Upper Body Torso Form with Removable Head, DisplayImporter, South El Monte, CA). The head was filled with Smooth-Cast® 60D shore cast urethane and has a weight of 5 kg to match the average adult head weight (Figure 3.3) (Yoganandan et al., 2009). The torso was filled with Portland Cement Type I/II and has a weight of 31 kg (Figure 3.4). Torso weight can be adjusted using static weights. The dummy neck is a single degree-of-freedom hinge joint

with two torsional springs in parallel (Figure 3.5). Additionally, bungee cords can be used to increase flexion stiffness. The torsional springs and bungee cords can be replaced to adjust the stiffness of the neck (Figure 3.6). The neck height can be adjusted using spacers.

The dummy is mounted on a base platform sled. The sled is mounted to bearings and rails to allow for translational motion along the direction of impact (Figure 3.7). The neck, head, and torso can be rotated and adjusted to alter the impact location on the helmet or to simulate front, side, and rear collisions. The dummy/sled can translate 1 m and sled motion is stopped using a dampening mechanism.

A youth-sized helmet and shoulder pads were purchased from Schutt Sports and sized to fit snugly on the dummy's head and shoulders. The head and helmet were instrumented with 3-axis accelerometers to measure the accelerations along the x, y, and z axes of the head and helmet. Accelerometers were also mounted to the shoulder pads and torso. The ADXL377 accelerometers have a dynamic range of 200G and a flat frequency response to 1.3 kHz for x and y axes and 1 kHz to z axis (EVAL-ADXL377Z, Analog Devices, Norwood, MA). The accelerometer sensitivity was measured by a ±1 g test and it was in a range of 5.8 to 7.2 mv/g. The biased voltage or offset was measured while the accelerometers were positioned on each part. The accelerometers sensitivity Acceleration and inclinometer data were collected using a compact RIO from National Instrument and a custom LabVIEW program.

3.2.3. Testing Protocol, Data Acquisition, and Analysis

Accelerometers were attached with adhesive-backed strips to the back of the head, top of the helmet, on the torso, and on the left-side of the shoulder pad in a way that they could not be damaged or detached during the experiment. The impact location was on the front of the helmet approximately 160 mm anterior and 200 mm superior from the center of the top neck plate. The

helmet position was marked on the head for repeatability. The chin strap was tightened to limit relative shift of the helmet and head. The sled system was positioned such that the head impact occurred when the pendulum arm was vertical. Each experiment was repeated five times, and standards deviations were calculated. Helmet acceleration rise time and contact duration of 4-6 milliseconds and 14-16 milliseconds, targeted based on the previous *in-vivo* studies. An aerospace-grade polyurethane foam material which had good restitution and minimal damping properties inserted between the steel face of the pendulum and ultra high molecular weight (UHMW) polyethylene cap to achieve the contact duration based on a previous study (Pellman et al., 2006).

The four impact energy levels were selected for the experiment based on the computational model and the literature. To reach the helmet peak acceleration of 10 to 20 g, which normally occurs in a football game (Rowson et al., 2009), a minimum impact energy level of A (≈ 6.6 J) with 20° drop angle was selected. In addition, two impact levels of B (≈ 25.4 J) and D (≈ 54.4 J) were chosen based on a previous pendulum study (Bartsch et al., 2012a). The impact energy levels were associated with dropping angles of 40° and 60° for the arm and 6.8 kg weight for the pendulum head, which were calculated in the computational model based on the conservation of energy. The drop angle of 50° or C impact level (≈ 38.8 J) was chosen based on the drop angle release to demonstrate how the acceleration curve moves with respect to the impact energy.

Neck spring stiffness was measured in a custom-built experimental setup (Figure 3.8). A stepper motor with a single line of action with a load cell in line was used to extend the head and neck from an initial zero position to 30°. Five cycles were performed for each set-up, and the data were averaged for all of the extension cycles of the neck. The angle of the neck was measured using an inclinometer mounted to the head, and the torque was determined using the measured

extension force and its line of action and moment arm with respect to the hinge joint center location. Neck stiffness was reported as a torque-rotation relationship.

3.3. Results

The purpose of the model simulations was to determine the necessary energy level and velocity in order to achieve a targeted peak head acceleration. By releasing the arm from a certain angle and with a certain weight and changing the neck springs stiffness, the impact on the neck was determined (Figure 3.9). However, adding dampers changed the peak acceleration, and the higher the damping coefficient the smaller the peak acceleration (Figure 3.10). Furthermore, while the pendulum head weight did not change the helmet or head peak acceleration (Figure 3.11), the drop angle had a great effect on peak accelerations (Figure 3.12). The computational model led to improvement of the impactor design and understanding of the critical design parameters.

The neck stiffness, shown as torque with respect to the head extension angle, is shown for three different configurations based on a custom-built experiment (Figure 3.13). The three stiffness levels were determined as Low, Medium, and High. In the experimental setup, drop angles were changed in the experiment in order to change the energy level. These impact energies resulted in different helmet and head peak accelerations (Figure 3.14 and Figure 3.15). Expectedly, the higher the impact energy the higher the peak acceleration observed with less than 2.1 g standard deviation in the experiments (Table 3.1). In the computational model, the springs stiffness of the neck (Figure 3.9) did not show any variations in the head acceleration. Consistently, the three neck springs' stiffness in the experiment did not influence the helmet and head peak acceleration, even though the head maximum acceleration occurred sooner while the neck had lower stiffness (Figure 3.16 and Figure 3.17). The standard deviation and peak accelerations of five trials acceleration demonstrated the insignificance of the stiffness and the repeatability of the experiment

(Table 3.2). In addition, comparing the helmet peak acceleration and the head maximum acceleration with respect to the level of impact energy exhibited an approximate of 10 g reduction for impacts up to 30 J, whereas this reduction decreases to about 5 g after 40 J impacts (Figure 3.18). By basic fitting a shape-preserving interpolant, the impact energy level of 36 J and 57 J showed 4.9% and 6.5% difference with respect to a previous study (Lewis et al., 2001). Furthermore, in all trials, the head peak acceleration occurred 5 to 7 milliseconds after the helmet was hit by the pendulum. Here, the padding works as a small spring-damper mechanism, which mitigates and distributes the force to the head. Consequently, the helmet through the deformation of the foam reduces the impact energy transmitted to the head, and slows the head to reach its peak 5 to 7 milliseconds later than the helmet.

3.4. Discussion

In this study, an impactor machine that can replicate helmet collisions experienced by football players was designed and built. A computational model of the impactor machine was developed to determine critical design parameters. The computational model demonstrated that the springs' preload and stiffness do not have a role in changing the peak acceleration which was verified by the experiment. In the computational model, the changes in the drop angle and the pendulum head weight indicated a different impact occurrence time (Figure 3.11 and Figure 3.12). However, the impactor is a compound pendulum which is a rectangular shaped arm with a weight at the end swinging by a pivot. In the compound pendulum both dropping angle and the pendulum head weight should be considered in addition to the length of the arm (Meriam and Kraige, 2012). The larger variation of the impact energy while the release angle was different demonstrated the need for altering the drop angle during the experiment to achieve a higher extent of impact energy levels. Based on the computational model, the impactor was designed in a way that it could achieve

the maximum level of 110 J impact energy which is about 50% higher than the energy level which causes concussion in football field (Bartsch et al., 2012a).

In a previous study, Bartsch et al. used a pendulum impactor and Hybrid III dummy and achieved 70 g and 120 g peak head accelerations for 25.4 J and 54.4 J impact levels, respectively (Bartsch et al., 2012a). In another study, Lewis et al. found 56.4 ± 1.0 g and 35.3 ± 2.0 g peak head acceleration for 57 J and 36 J impact levels using intracranial accelerometers (Lewis et al., 2001). While the neck strength and mobility is an important parameter in the peak acceleration calculation, comparing previous studies might help us to improve the construction of the dummy and the impactor to reach a more robust design. In this study, the impact levels of 25.4 J and 54.4 J resulted in approximately 32.7 g and 64.2 g helmet peak accelerations, and 24.1 g and 58.4 g head peak accelerations for the neck, respectively, with the high neck stiffness level. The head peak acceleration shows 4.9% and 6.5% difference with regard to the Lewis et al. study which is in an acceptable range. However, the large difference with regard to Bartsch et al. study could be because of the impact locations or different neck designs. The impact location in the Bartsch et al. study is the maxillar-mandibular region; however, in this study the cerebrum or frontal region was hit, thus the moment arms are different and the energy is distributing differently. In the Hybrid III dummy, the neck is replicated by a deformable body, consisting of butyl rubbers and steel plates, in a way that it shows various stiffness and damping properties in different directions. Also, the rubber material in Hybrid III is distributed asymmetrically and consisted of a horizontal cut through the rubber along the front of the neck between each of the steel disks to replicate the asymmetric flexion/extension stiffness that observed in the human (Spittle et al., 1992). In this study's neck design, the neck joint was simulated as a hinge joint which can only reproduces

rotations, and the torsional springs and bungee cords were only able to simulate the stiffness of the neck and not the damping characteristics of it.

To understand the correlation between concussion and head acceleration, the relationship between helmet peak acceleration and head peak acceleration was studied after collisions (Figure 3.18). While the head peak acceleration occurs 7 milliseconds after the collision for impacts with less than 30 J energy, the head peak acceleration happens in 5 or 6 milliseconds after the impacts with energy levels of more than 30 J, which demonstrates shorter contact duration time. Also, during the experiments it was acknowledged that the chin strap has a great role in acceleration curve shape and peak. Testing the helmet without the chin straps showed a large helmet motion relative to the head, which resulted in a lower peak acceleration with two distinct peaks. Loosening the chin strap resulted in slight movement of the helmet and larger peaks for the head and helmet. Finally, a tight chin strap resulted in approximately no relative movement of the helmet. In this study, the results were shown and evaluated for the tight chin strap to show the worst situation for head acceleration.

The neck characteristics are dependent upon the players' age and their muscle tone. Also, when athletes brace their neck for impact, the stiffness and dampening characteristics of the neck change. Having a dummy with a customizable neck design allowed the neck stiffness to be evaluated, although it did not have a significant role in reducing the peak acceleration for the helmet and head. Since the generated force by the springs is dependent upon the displacement of the springs ($F = K\Delta x$), and the displacement of the system during the first 4 to 10 millisecond of the impact is negligible, the force cannot be large enough to reduce peak acceleration. In this study, the springs used for the neck have 2.06, 7.24, and 18.19 Nm moments at 1° head extension, while the Hybrid III neck has the 9.71 Nm moment at 1° head extension (Spittle et al., 1992). Since there

is no standard for designing the neck in football testing, the neck parameters are compared to the Hybrid III dummy which was created based on the experimental data of an average male person in the US (Mertz and Patrick, 1971). There was not any study found on the physical neck parameters of a braced neck, but this study confirmed that even doubling the neck stiffness does not change the head maximum acceleration significantly. The neck has dampening characteristics as well (Mertz and Patrick, 1971; Spittle et al., 1992). Since dampers generate force based on the change in velocity ($F = C\Delta V$), the damper was included in the computational model, and that revealed significant changes in the peak acceleration by changing the damping coefficient (Figure 3.10). Future studies need to evaluate the results experimentally and validate the effects of the dampers on the head maximum accelerations.

In the study, the impact velocity and the head velocity after the impact have not been investigated. Changes in the mass of the pendulum can vary the velocity of the head after the impact ($mV = const.$). To enhance the impact replication, the mass of the pendulum needs to be adjusted based on the literature. The neck was simulated by two torsional springs and bungee cords; however, no damping agents were used. More accurate springs and dampers could be added to the model to generate a more realistic neck; however, there is a lack of a standard for the neck mechanism or dummy simulations. In this study, only the helmet collisions were replicated, but the direct impact to the helmet are discouraged among the players and are against the NFL rules. Assuming that a helmet has the same ability to moderate energy generated from an impact regardless of the impact locations like on the faceguard or shoulder pad, the results may not change.

3.5. Conclusion

A machine for replicating the helmet collisions in the field was designed, built, and tested using various impact energy levels. The impact contact duration, rise time, and the acceleration

curves were targeted based on previous studies. As another specific aim of the study, the neck stiffness's influence on the peak acceleration was considered. The simulated collisions demonstrated that the neck stiffness does not change the peak helmet acceleration significantly. It was quantified and demonstrated that the helmets have larger head acceleration, although the helmet acceleration rise time is less than that of for head acceleration.

In a future study, as far as computational modeling is considered, the actual neck stiffness based on the torque-angle curve needs to be imported in the Adams model as spline at the neck hinge joint location. By choosing a certain impact energy, the contact properties can be modified between the pendulum head and the head. The goal is to achieve a similar helmet peak acceleration in a similar window of its rise time. Having the modified contact properties, the model can be justified and verified for the experiment. Consequently, using computational model, side impacts, dampening of the neck, pendulum weight variations to look at the impact of the head velocity, and other studies could be run.

Modifications can be made to improve the simulation for future studies. Adding a customized damper to the neck can modify the neck mechanics. In this study, only one helmet was used from Schutt Inc.; however, different helmets could be put on the dummy to test the padding differences. Simulating different impact locations, different lines of action for springs, or even simulating different frictions on the sled, could show interesting results in the future. Moreover, if a new helmet or shoulder pads are produced, the machine is able to validate and investigate the advantages or disadvantages of that design qualitatively and quantitatively.

Table 3.1. Standard deviation and peak accelerations for different energy level impacts

Energy Level	Neck Stiffness	Helmet Peak Acceleration (g*)	Standard Deviation for Helmet (g)	Head Peak Acceleration (g)	Standard Deviation for Head (g)
A	High	15.5	1.0	9.2	0.7
B		32.7	1.1	24.1	1.5
C		50.6	0.9	45.2	1.2
D		64.2	2.1	58.4	1.9

*g is gravity

Table 3.2. Standard deviation and peak accelerations for different stiffness level impacts

Energy Level	Neck Stiffness	Helmet Peak Acceleration (g*)	Standard Deviation for Helmet (g)	Head Peak Acceleration (g)	Standard Deviation for Head (g)
B	Low	33.4	1.7	25.3	1.0
	Medium	33.6	2.4	25.6	2.0
	High	32.7	1.1	24.1	1.5

*g is gravity

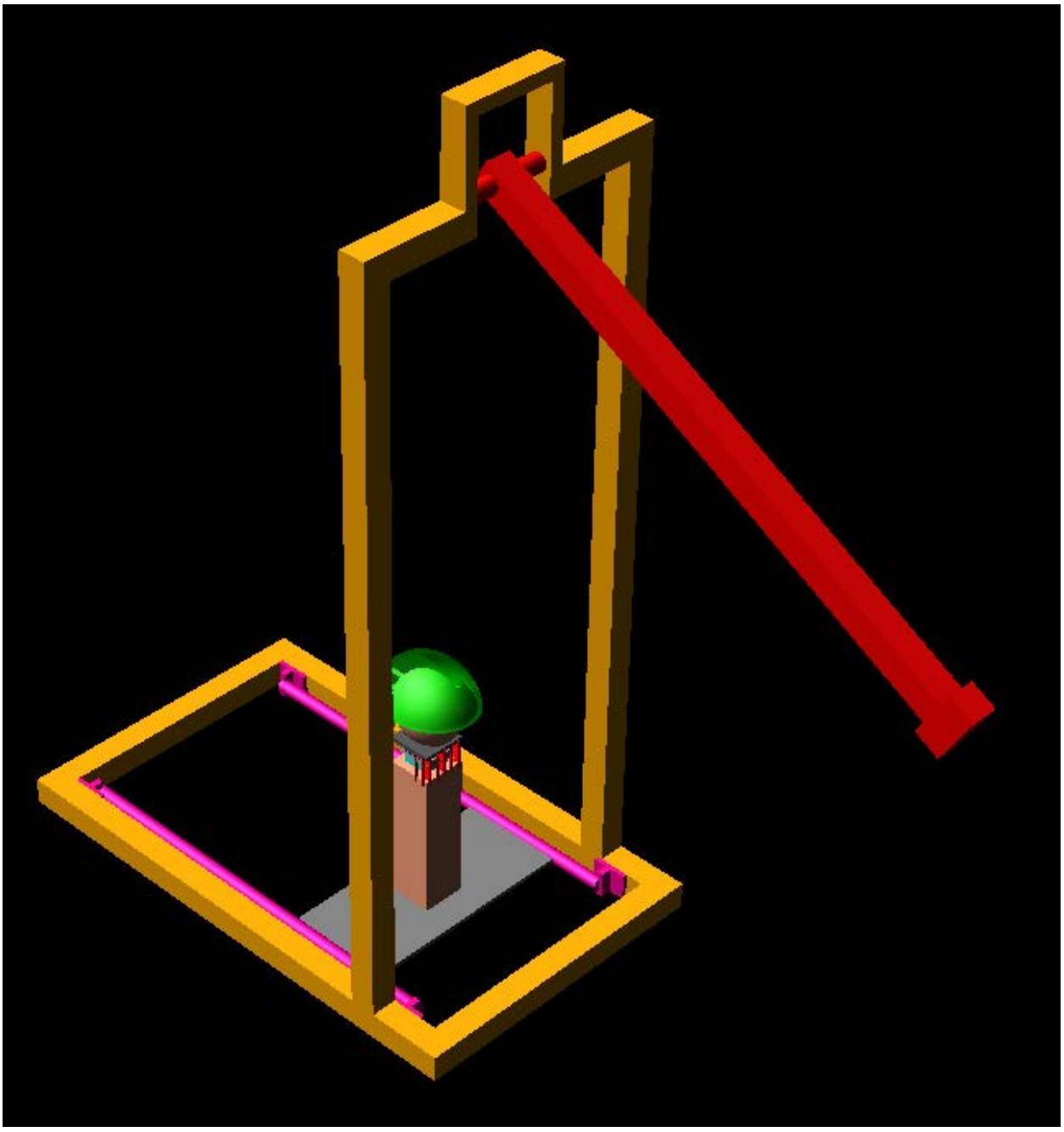

Figure 3.1. The isometric view of the impactor computational model

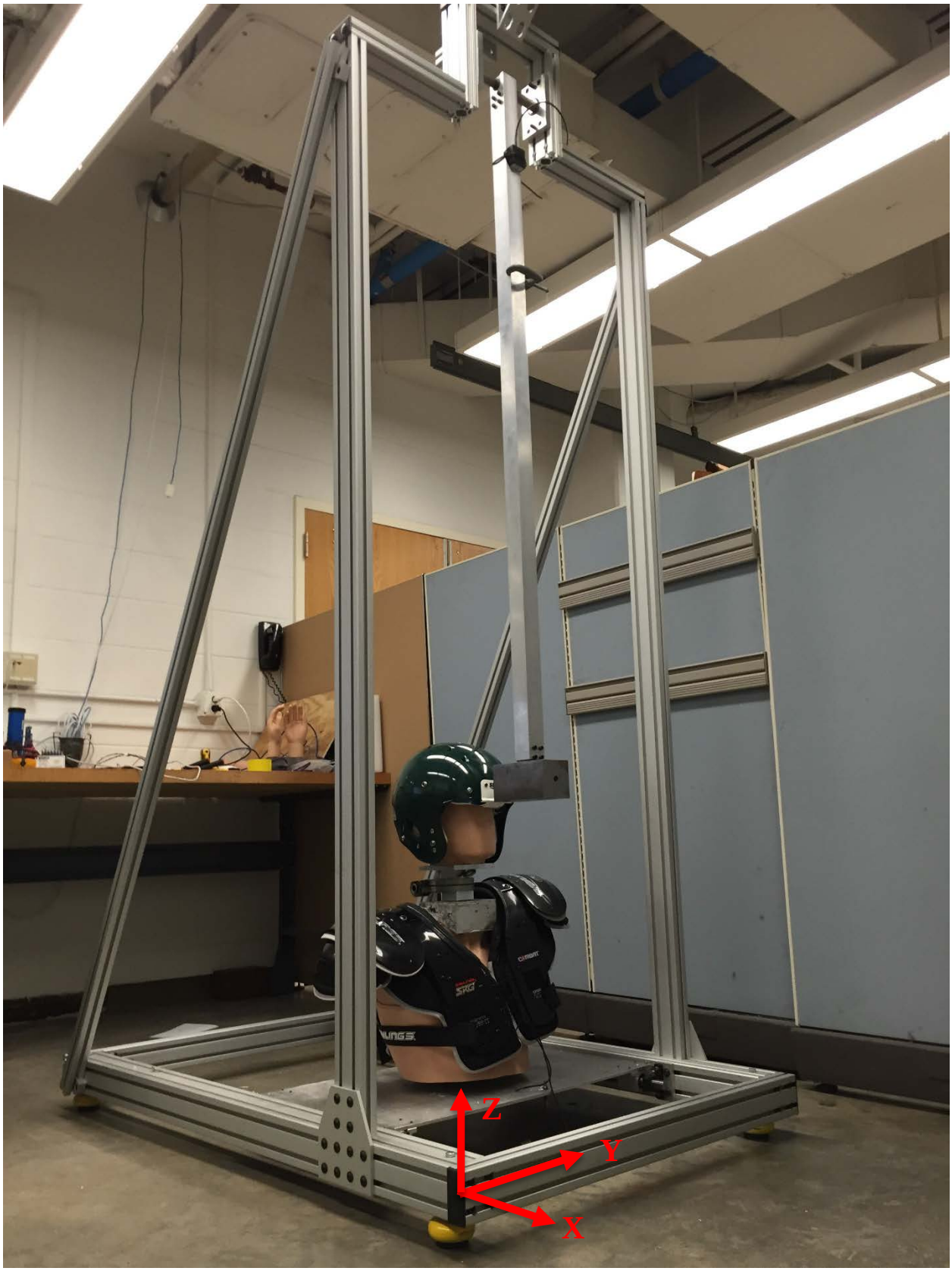

Figure 3.2. The impactor

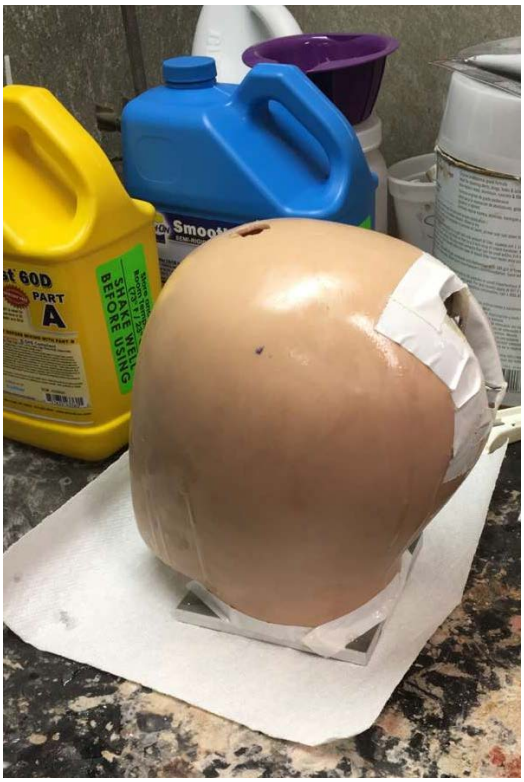

Figure 3.3. Mannequin head filled with Smooth-Cast® 60D shore cast urethane

Figure 3.4. Mannequin torso filled with Portland Cement Type I/II

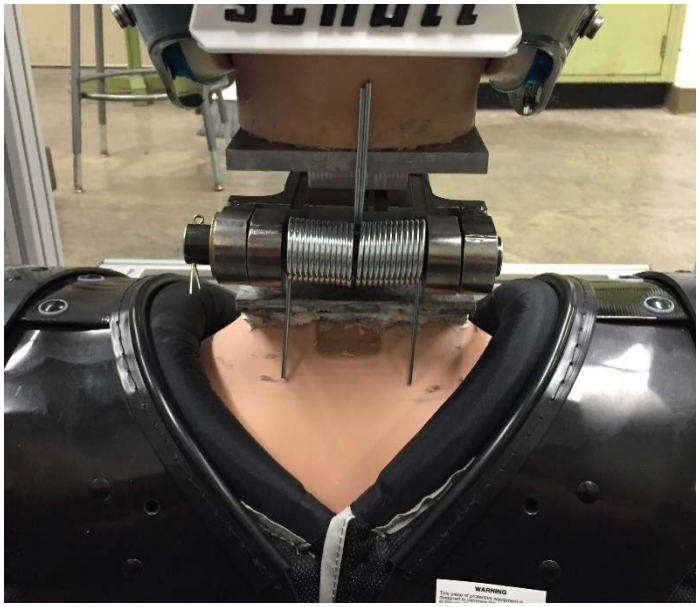

Figure 3.5. Neck with torsional springs in series

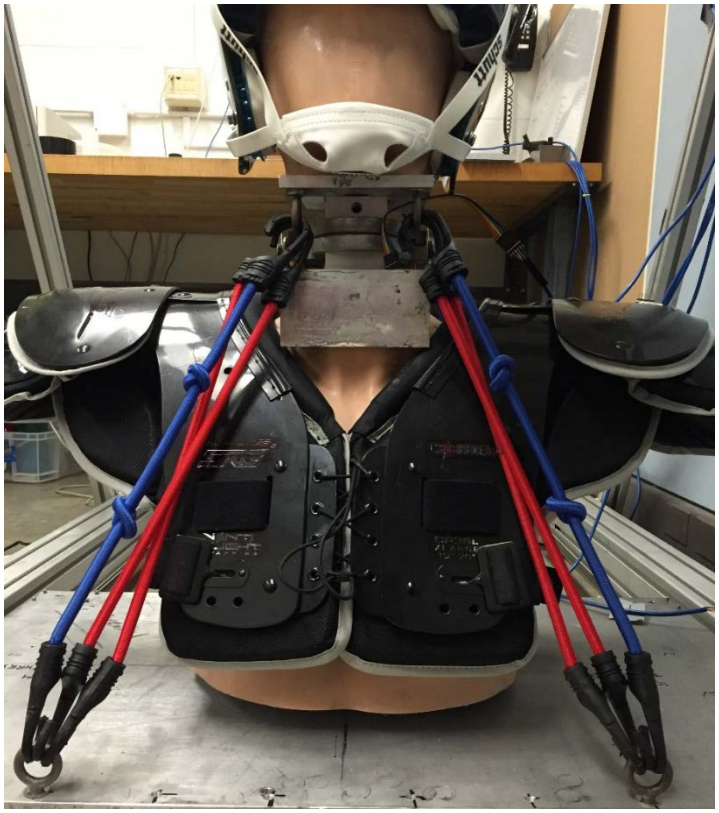

Figure 3.6. Bungee cords used to generate neck stiffness

Figure 3.7. Slider system

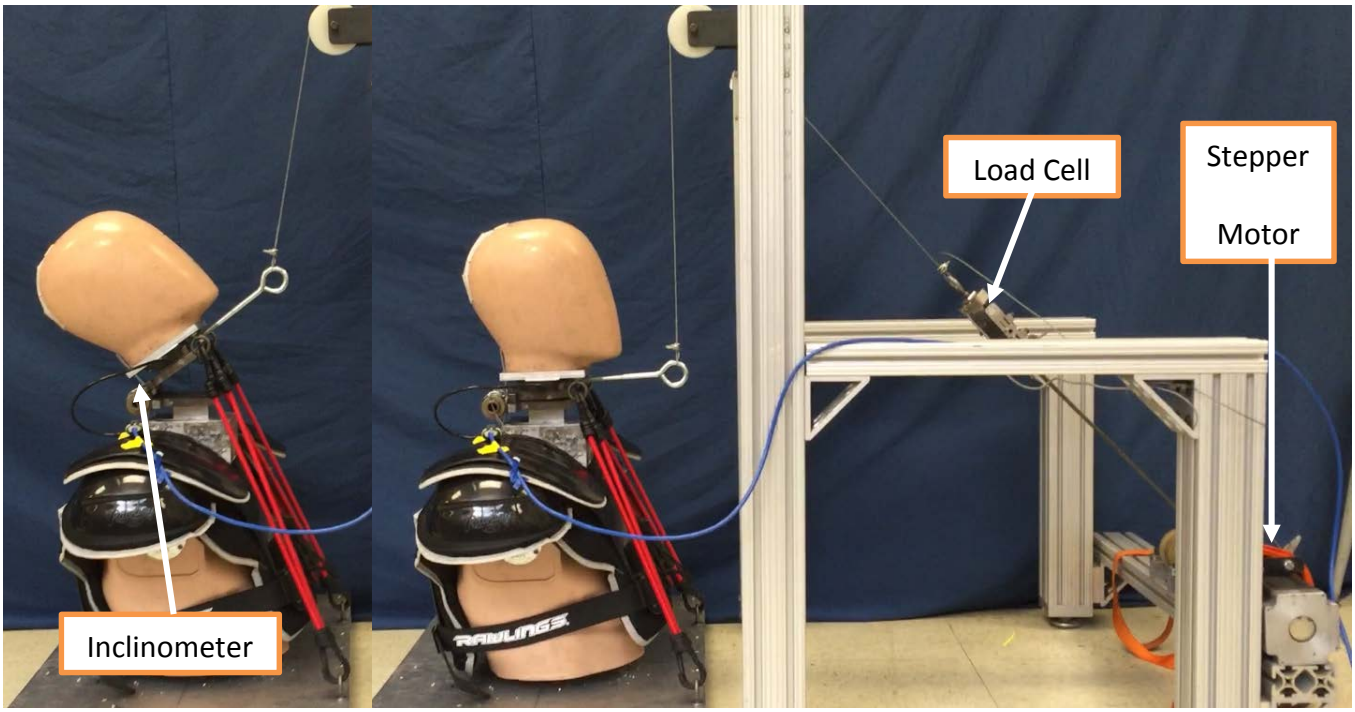

Figure 3.8. Stiffness measurement experimental setup

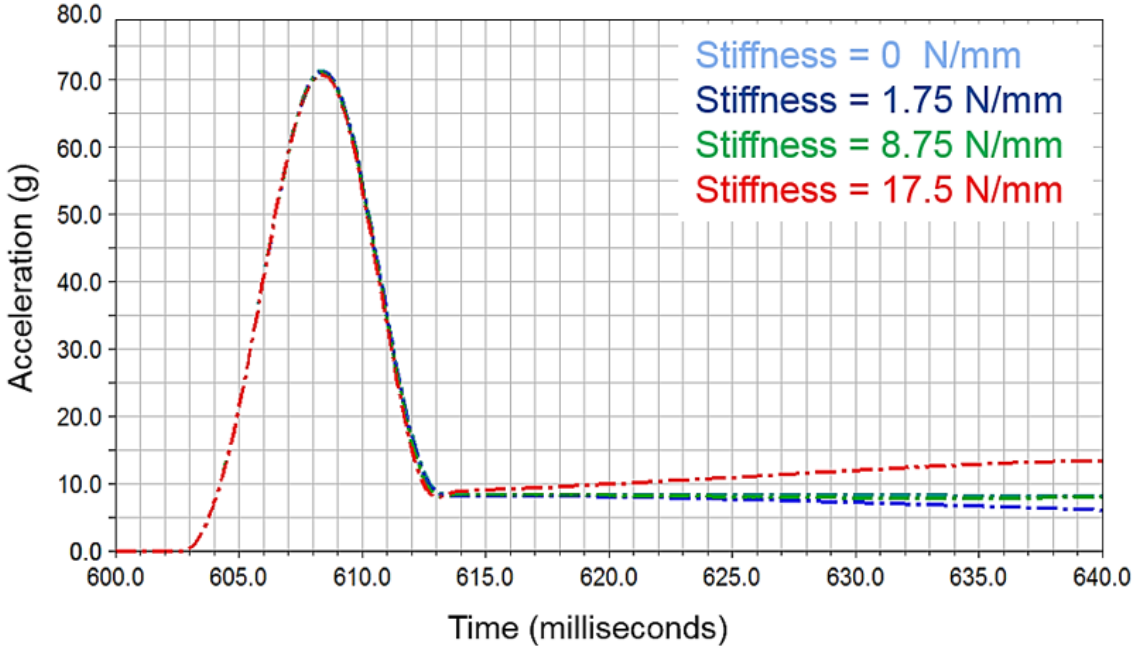

Figure 3.9. Neck spring stiffness effect on the acceleration curve (Computaitional Model)

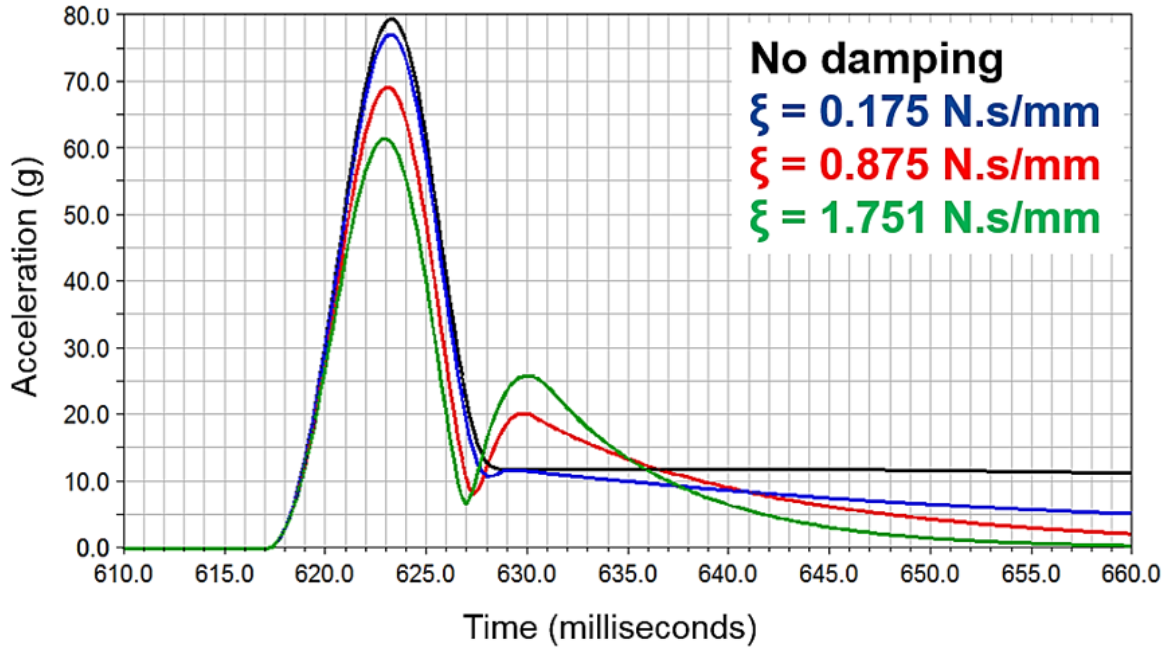

Figure 3.10. Damper coefficient effect on the acceleration curve (Computaitional Model)

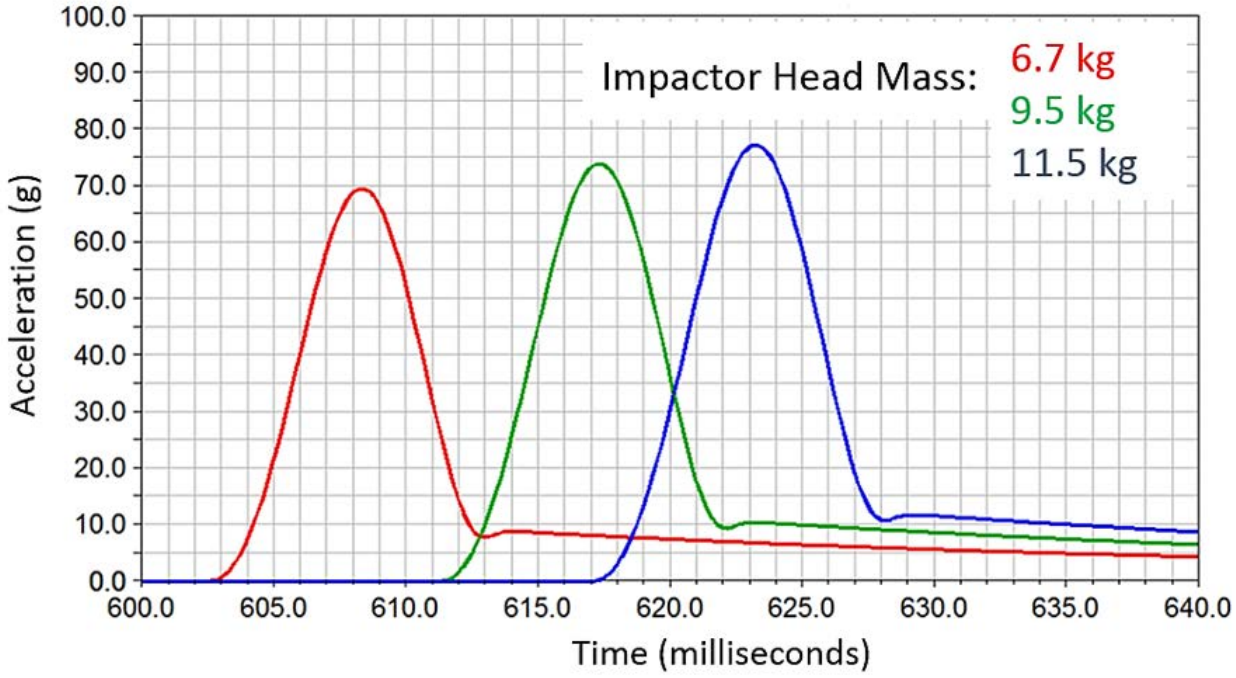

Figure 3.11. Impactor head mass effect on the acceleration curve (Computaitional Model)

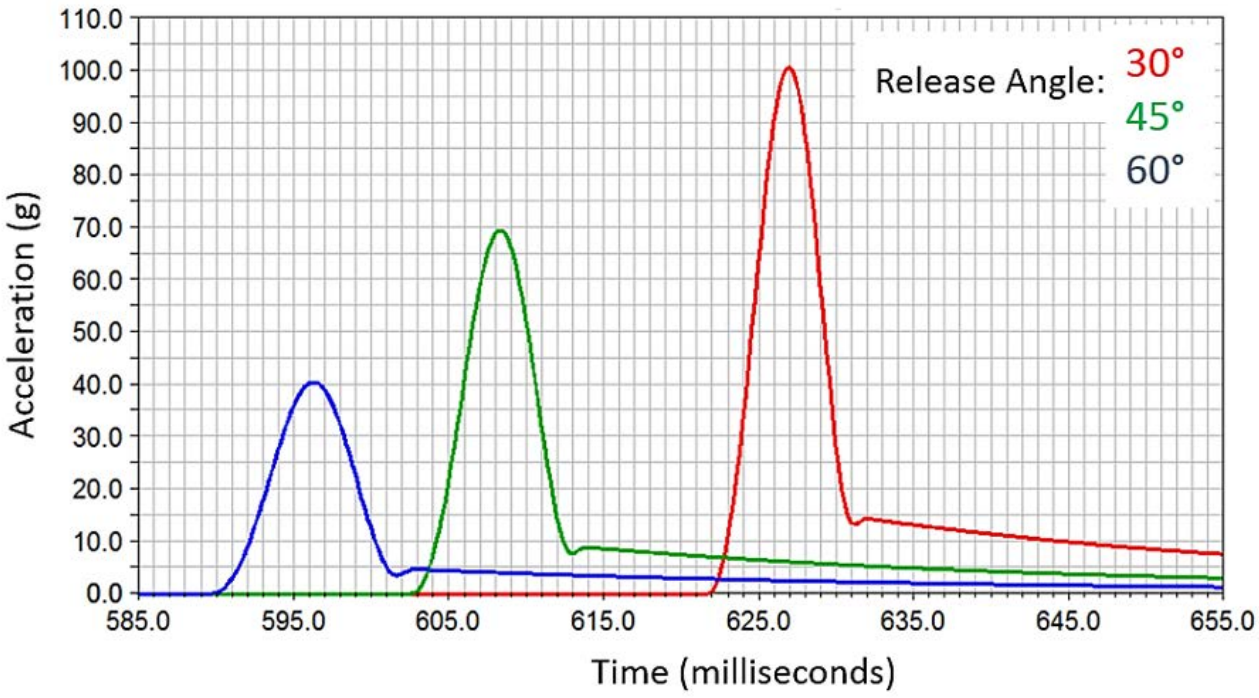

Figure 3.12. Impactor drop angle effect on the acceleration curve (Computaitional Model)

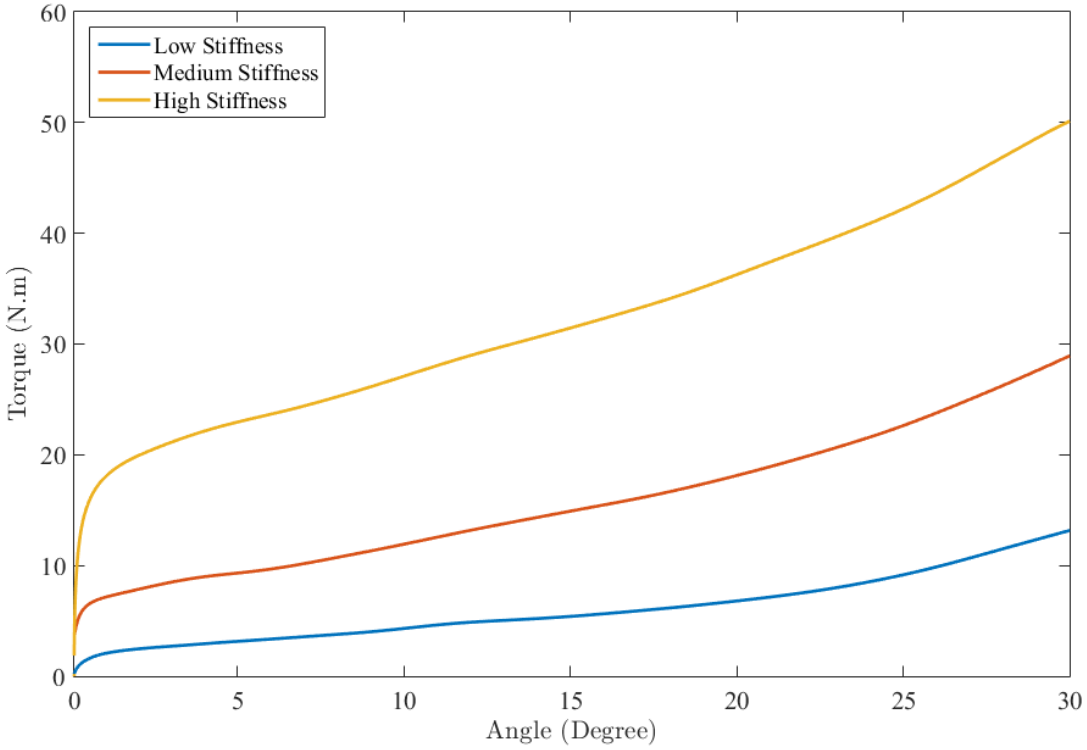

Figure 3.13. Neck stiffness

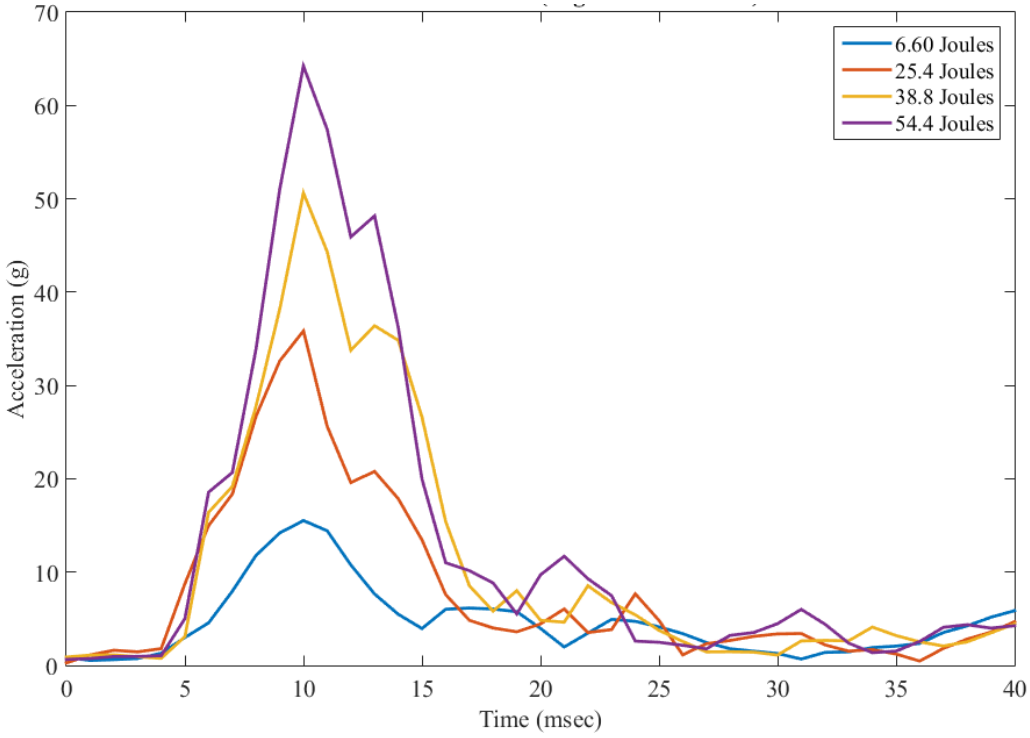

Figure 3.14. Helmet acceleration curve versus the impact energy level

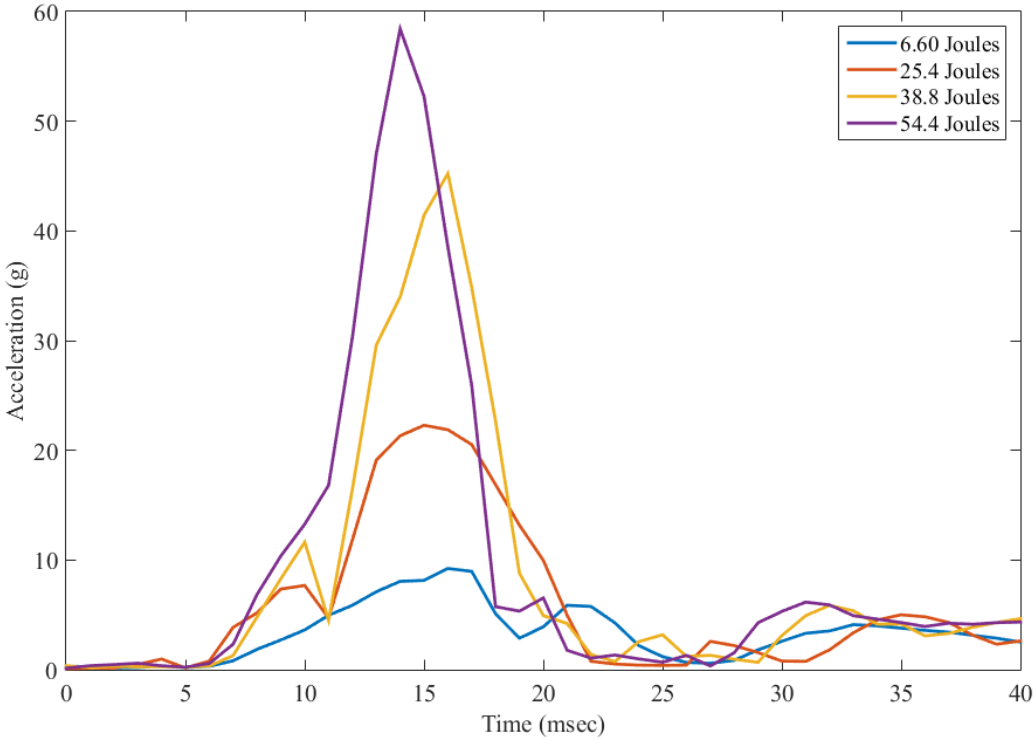

Figure 3.15. Head acceleration curve versus the impact energy level

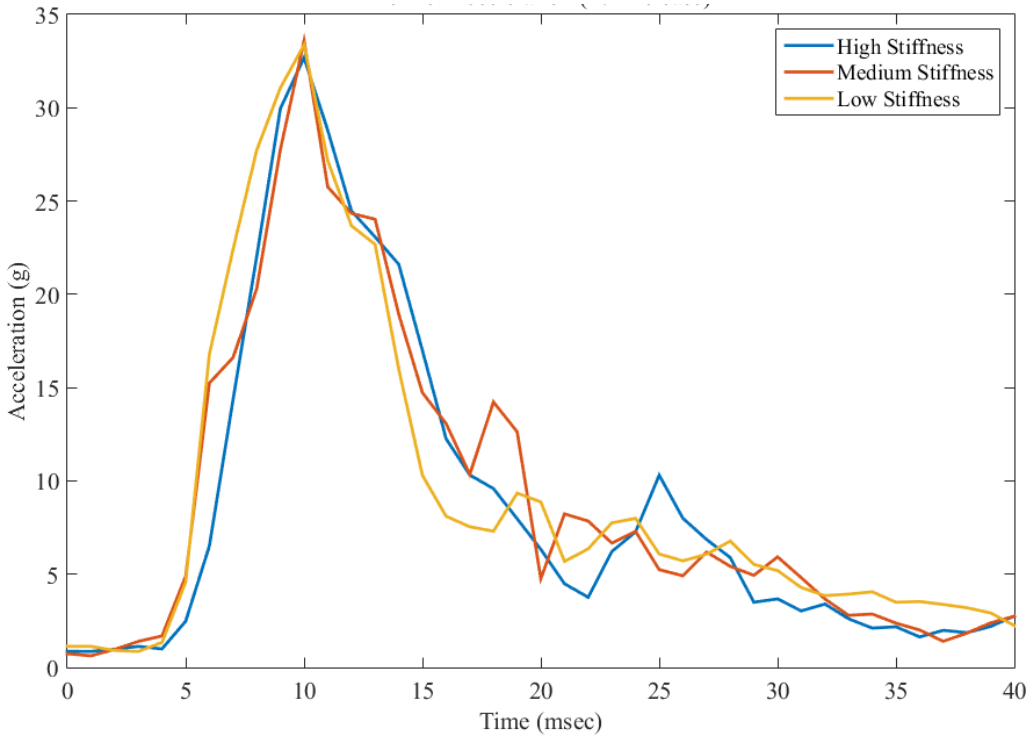

Figure 3.16. Helmet acceleration curve based on different neck stiffness

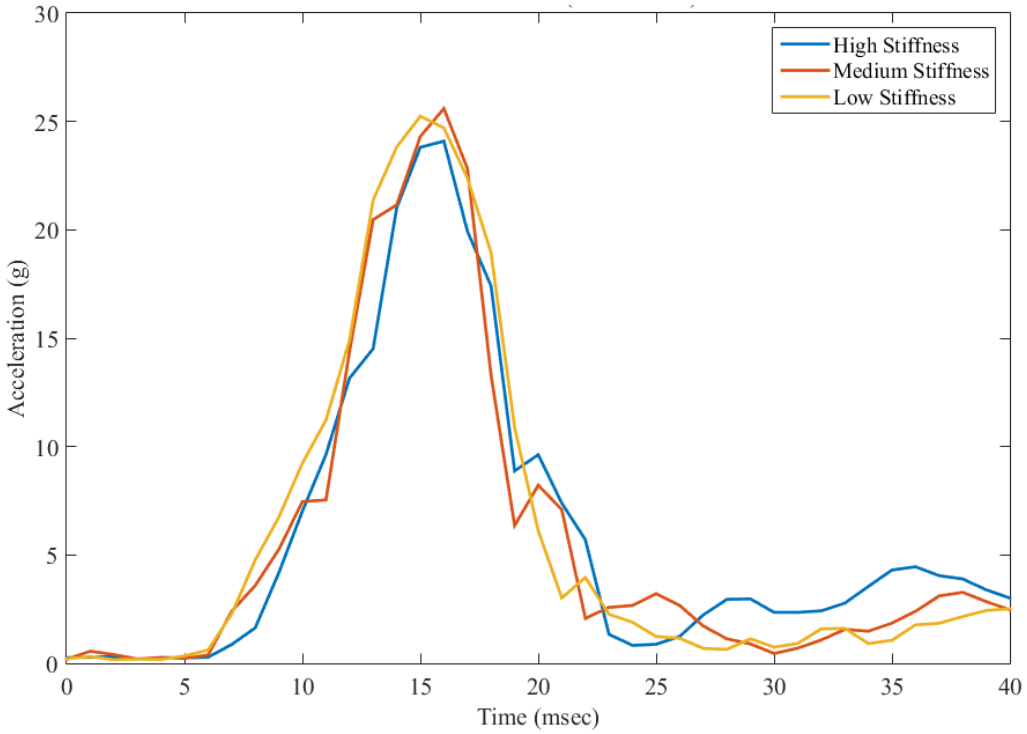

Figure 3.17. Head acceleration curve based on different neck stiffness

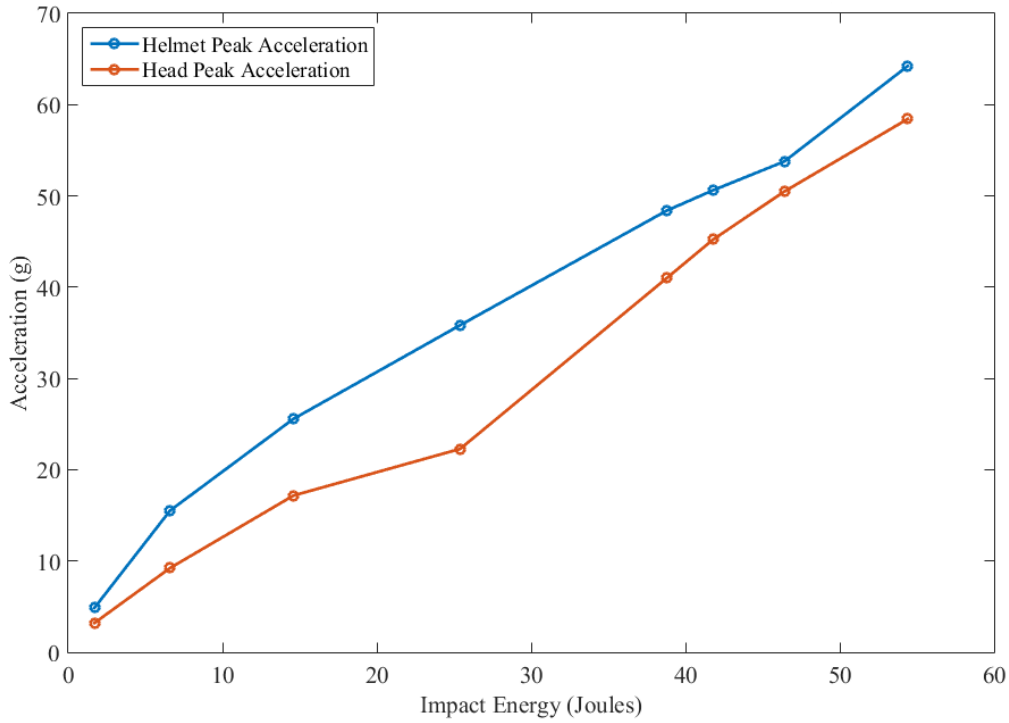

Figure 3.18. Peak helmet and head accelerations with respect to the impact energy level

4. Ankle Anatomy and Injuries

This chapter is separated into two fundamental categories of anatomy and injury. Anatomy section briefly discusses the bones, muscles, tendons, and ligaments around the ankle joint complex which are important in our study. Injury section concisely dicusses the common ankle joint injuries and how they occur.

4.1. Anatomy

4.1.1. Bones

The ankle joint complex is comprised of four connected bones: tibia, fibula, talus, and calcaneus (Figure 4.1) (Payne et al., 1997). The tibia affords load bearing transmission between the ankle and the upper body parts. The fibula is mainly used for muscle and tendon connection. The talus is connector of tibia and fibula to the calcaneus and forefoot. The calcaneous delivers skeletal support for the foot and it is the heel of the foot.

4.1.2. Ligaments

The collateral ligaments of the ankle joint complex (AJC) consists of the anterior talofibular ligament (ATFL), the posterior talofibular ligament (PTFL), and the calcaneofibular ligament (CFL). In general, these ligament maintain the stability of the ankle joint (Burks and Morgan, 1994) (Figure 4.2). The ATFL, according to *in-vitro* kinematic experiments, prevents anterior shift of the talus from the mortise and unnecessary inversion and internal rotation of the talus on the tibia (Burks and Morgan, 1994; Hertel, 2002). While both the inversion and internal rotations in the loaded talocrural joint are constrained by the PTFL, the studies showed that the CFL limits unnecessary inversion and internal rotation of the rear-foot. Clinically, the ATFL and CFL are the most important to sustain the stability and oppose the laxity of the ankle in inversion

movements. The strain of the ATFL has been shown to increase as the ankle plantarflexes, while the CFL reaches its highest strain in dorsiflexion (Hertel, 2002).

4.1.3. Muscles and Tendons

The relevant tendons in the ankle joint complex are tibialis anterior tendon (TA), and extensor digitorum longus tendon (EDL) which are linking the muscles with the same name to the calcaneus (Figure 4.3). The TA is responsible for nearly 80% of the dorsiflexion in the ankle (Gallo et al., 2004), while the EDL is the only muscle which contributes in everting the ankle and dorsiflexing it (Pointinger et al., 2003). Moreover, Achilles tendon attaches the gastrocnemius muscle to the calcaneus and is the main extensor of the AJC.

4.2. Ankle Ligament Injuries

The ankle can be injured in various ways, but the most common sports injury of the AJC is ankle sprain, and more than three quarter of the ankle sprains are lateral injuries (Hertel, 2002). Ankle sprains can be categorized into three grades, based on their severity (Figure 4.4). Grade I is characterized as a mild stretching or partial tear to a collateral ligament, mainly ATFL or CFL. There is usually very little functional loss following Grade I injury. Grade II is a partial rupture of the ATFL usually with moderate pain which causes functional limitations and a minor to moderate instability. Grade III sprains are rare and occur when the ligaments are fully severed (Petersen et al., 2013). This type mostly needs a fixation of the ankle or surgical intervention.

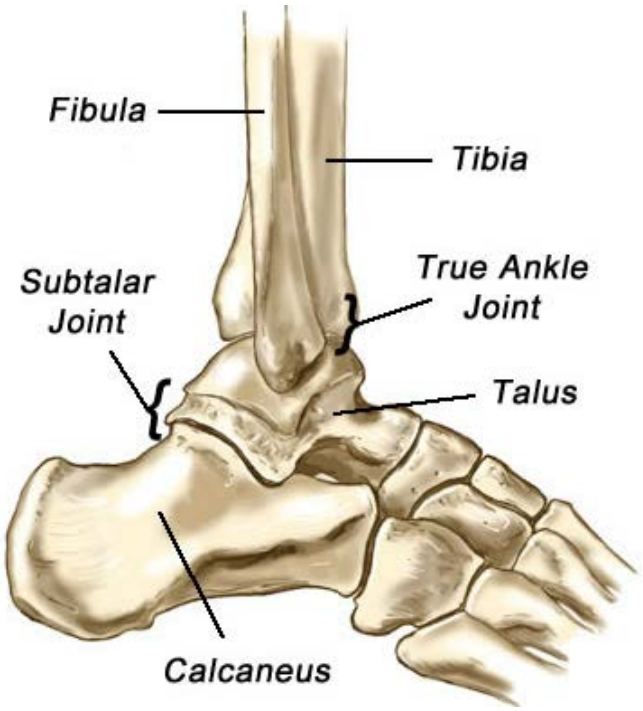

Figure 4.1. Bones in the ankle: Tibia, Fibula, Talus, and Calcaneus (Kidport, 2016)

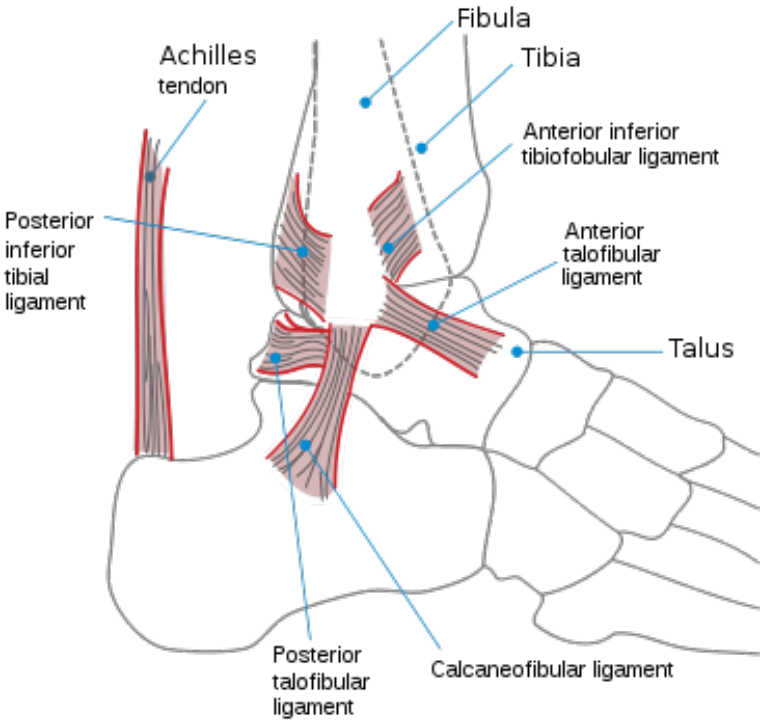

Figure 4.2. The collateral ligaments of the ankle joint (Louisvilleorthopedics, 2016)

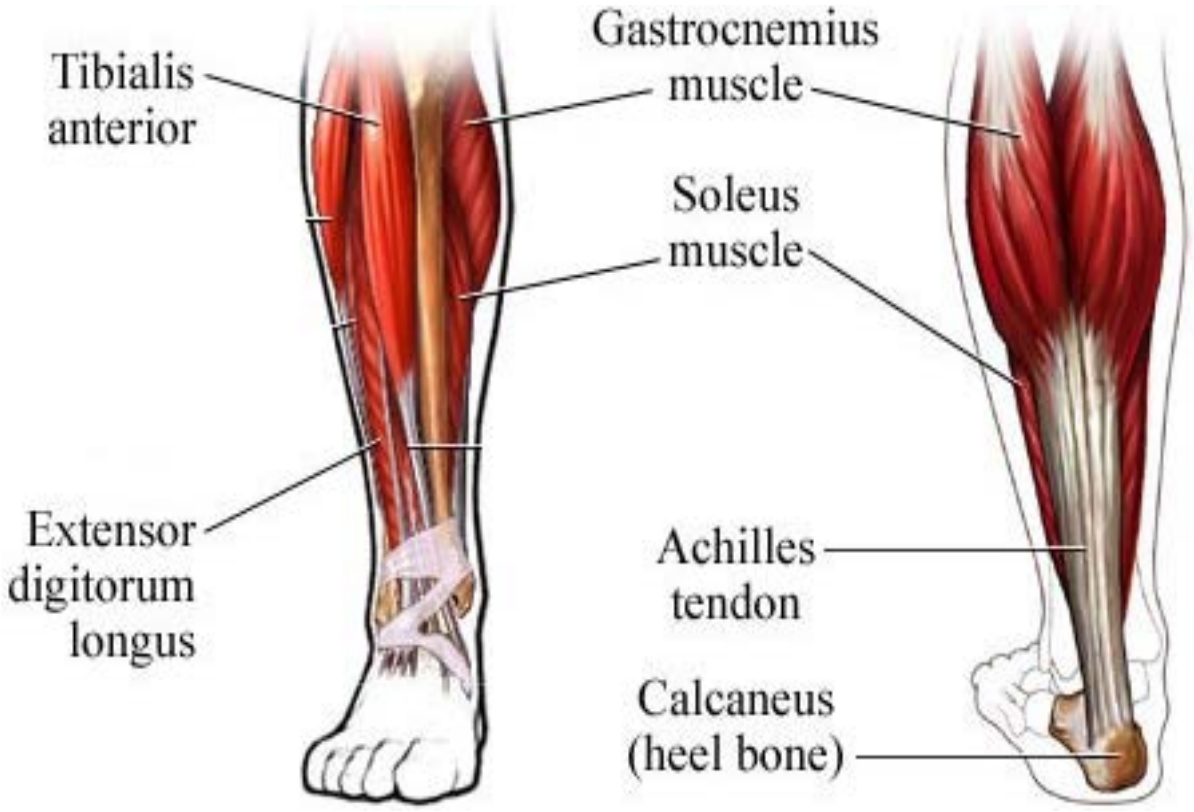

Figure 4.3. Ankle muscles and tendon anatomy (AnatomyCharts, 2016)

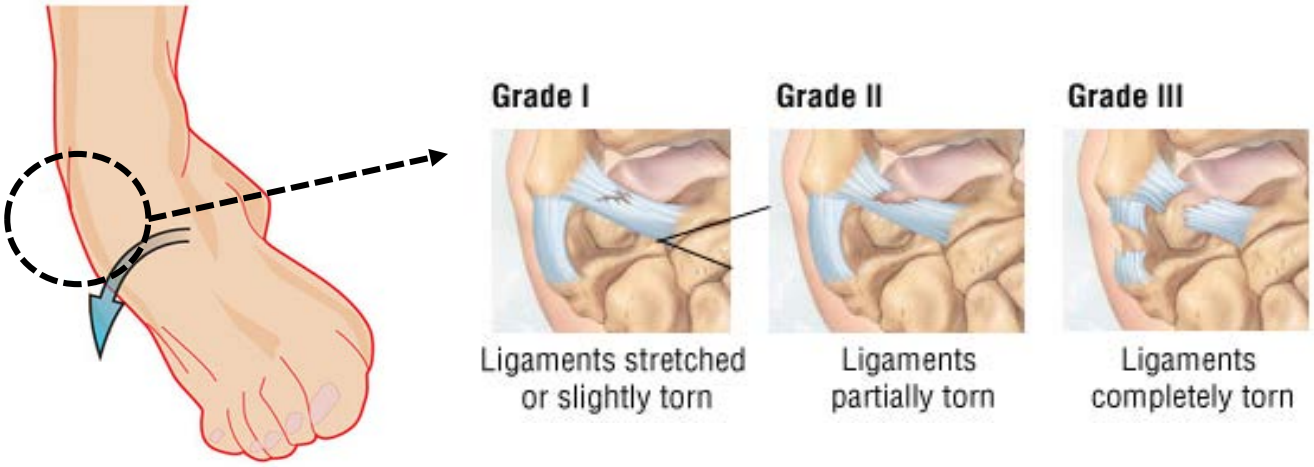

Figure 4.4. Different injury grades in inversion and adduction (DocPods, 2016)

5. Changes in the Biomechanics of the Ankle Joint Complex after Injury and Effects of Muscle Contribution

5.1. Introduction

Injuries to the ankle joint are one of the most common sports injuries (Payne et al., 1997). Inversion injuries cause by rupture or sprain in collateral ligaments lead to joint instability and account for more than 80% of ankle injuries (Brooks et al., 1981; Brostroem, 1964; Slimmon and Brukner, 2010). Moreover, changes in the muscle activity have been seen after the injuries and their subsequent rehabilitation (Beckman and Buchanan, 1995). Thus, the main muscles of the foot (the gastrocnemius, soleus, tibialis anterior, and extensor digitorum longus) will be activated differently after the joint rehabilitation (Murphy, 1983). Understanding the effects of collateral ligaments after the injury as well as muscle contribution might be helpful for developing rehabilitation techniques and making the diagnosis procedure more accurate.

The collateral ligaments of the ankle joint complex (AJC) consists of the anterior talofibular ligament (ATFL), the posterior talofibular ligament (PTFL), and the calcaneofibular ligament (CFL). In general, these ligaments maintain the stability of the ankle joint (Burks and Morgan, 1994). The ATFL, according to in-vitro kinematic experiments, prevents anterior shift of the talus from the mortise and unnecessary inversion and internal rotation of the talus on the tibia (Burks and Morgan, 1994; Hertel, 2002). While both the inversion and internal rotations in the loaded talocrural joint are constrained by the PTFL, the studies showed that the CFL limits unnecessary inversion and internal rotation of the rear-foot. Clinically, the ATFL and CFL are the most important to sustain the stability and oppose the laxity of the ankle in inversion movements. The strain of the ATFL has been shown to increase as the ankle plantarflexes, while the CFL reaches its highest strain in dorsiflexion (Hertel, 2002).

Based on their severity, there are three grades or types of ankle ligament sprains. Grade I is characterized as a mild stretching or partial tear to a ligament. Grade II is a partial rupture of the ATFL, usually with moderate pain which causes functional limitations and a minor to moderate instability. Grade III sprains occur when the ligaments are fully severed (Petersen et al., 2013).

Moreover, the relevant tendons in the ankle joint complex are the tibialis anterior (TA) tendon and extensor digitorum longus (EDL) tendon which link the muscles with the same name to the calcaneus. The TA is responsible for nearly 80% of the dorsiflexion moment in the ankle (Gallo et al., 2004), while the EDL is the only muscle which contributes in both everting and dorsiflexing the ankle (Pointinger et al., 2003). Moreover, the Achilles tendon attaches the gastrocnemius muscle to the calcaneus and is the main extensor of the AJC.

Most cadaveric studies of the AJC investigate only the passive kinematics of the AJC without simulating loads on anterior tendons and muscles which leads to a more physiological response. One study simulated both anterior and posterior compartment muscle loads to evaluate the natural kinematics within plantarflexion and dorsiflexion motion, but did not evaluate the injury (Stahelin and Weiler, 1997). Weindel et al. studied the effects of rupturing each ligament by generating a constant moment on the foot without any loadings on the other tendons (Weindel et al., 2010). Accordingly, there is a lack of literature describing AJC kinematics before and after the ankle injuries while mimicking muscle loads. Having static loads on muscles allows examination of a more physiological behavior of the joint. Also, in-vitro simulation of in-vivo loading sets of muscles provides an ability to achieve practical results which could be related to clinical outcomes, such as improvement of implants and rehabilitation programs after the surgery, for both normal and pathological conditions. Additionally, similar to joints like the shoulder or knee, ankles have also been shown to be highly susceptible to subsequent injury, and ankle injury

is the strongest predictor of future ankle sprains (Engebretsen et al., 2010; McKay et al., 2001). This is often due to incomplete or ineffective repair and therapy (Devries et al., 2011; Mizel et al., 2004). Rehabilitation programs and injury diagnosis can be improved by understanding the effects of muscle weakness on the kinematics.

Quantifying the effects of the tibialis anterior and extensor digitorum longus on the ankle joint complex will aid in muscle function analysis after injury by determining the effects of muscles weakness on the ankle joint kinematics. The first aim of this study was to measure the effect of variable muscle loading configurations on the ankle joint complex kinematics. The second aim was to quantify the effects of ankle sprain on the ankle joint biomechanics under a muscle-loaded condition.

5.2. Materials and Methods

Nine cadaveric ankles (7 male, 5 right) with an average age of 57 years (range 49-73) and BMI of 26.0 (range 18.0-35.0) were used in this study. No history of degenerative bone disease or previous ankle injury was reported for any specimen. Full leg specimens were obtained frozen, thawed, sectioned mid-tibia, and refrozen. Specimens were later thawed at room temperature for at least 18 hours prior to testing. All soft tissue more than 6.5 cm superior to the medial malleolus was resected except for the TA, EDL, and Achilles tendons which were clamped independently, and their line of actions were constrained by the skin. Adhesive putty secured an aluminum fixture that was centered on the tibia. The ankle was then mounted onto an open chain muscle loading rig with the tibia rigidly attached in an inverted, vertical position and the foot free to move (Figure 5.1). The ankle was flexed three times over the entire range of flexion using a Nema 34 stepper motor (Danahar automation, Illinois) attached to the Achilles tendon. The stepper motor ran in position control having the pattern of triangular wave with smooth edge. The fully-

dorsiflexion and fully-plantarflexion was determined based on virtual feedback. Post-processing was done for the second cycle. Static loads were applied to the TA and the EDL using dead weights.

Bony landmarks on the tibia were probed to create a body-fixed coordinate system. The body-fixed coordinate system for the calcaneus was defined so that it was coincident with the tibial coordinate system in the neutral position. The neutral position was defined while the AJC had zero degree dorsi-plantarflexion, internal-external rotation, and inversion-eversion. All kinematic measures were described with respect to this neutral position. The two body-fixed coordinate systems were used to calculate the AJC kinematics using a modified 3-cylindrical open-chain description of kinematics (Grood and Suntay, 1983; Wu et al., 2002). The kinematics of each bone were measured using iRED markers rigidly attached to the calcaneus and the tibia using an Optotrak Certus motion capture system (Northern Digital, Ontario). The loads applied by the motor onto the Achilles tendon to dorsiflex and plantarflex the ankle were measured using a 1200 N load cell (Transducer Technique, Temecula, CA).

5.2.1. Biomechanics of Muscle Contributions

Three loading conditions were simulated in this aim: physiological loading defined as 90N on the TA and 45N on the EDL based on their physiological cross sectional area (PCSAs) (Arnold et al., 2010), the second load set was defined as Weak TA or Strong EDL (Weak TA) which reduced the TA load from the physiological set to 75% and increased the EDL load 150%, and the third load set defined as Weak EDL or Strong TA (Weak EDL) which reduced the EDL load to 50% of the physiological cycle and increased the TA load to 125% (Table 5.1). Total static load on the tendons remained 135 N during the load sets. The physiological load set was used as the baseline for comparison.

5.2.2. Biomechanics of the Injury

In this aim, similar to the previous aim, static loads were used to load the TA and the EDL. The physiological loading set was defined as 90N on the TA and 45N on the EDL based on their PCSAs (Arnold et al., 2010). A severe Grade II injury was simulated by resecting only the ATFL followed by a resection of the CFL to simulate a severe Grade III injury. After simulation of the injury and dissection of the ligaments, the skin and muscle were sutured to restrict excessive movement of the AJC. The intact ankle was used as the baseline for comparison.

5.2.3. Data Analysis

Kinematic data were approved for normal distribution post analysis according to the normal probability distribution plot and Anderson-Darling test with five percentile confidence interval. The sagittal plane flexion kinematics were normalized to percent of maximum dorsiflexion and percent of maximum plantarflexion to account for variation in total flexion range that was not consistently divided between plantarflexion and dorsiflexion (Table 5.2). Kinematic and load data were filtered with a low-pass digital Butterworth filter with normalized cutoff frequency of 0.1 Hz to eliminate the noise in the system. Analysis was restricted to extension cycles (maximum dorsiflexion to maximum plantarflexion) to avoid hysteresis in load through the Achilles tendon. For all protocols, the means and standard deviations were calculated individually. Using anova_rm toolbox in MATLAB 2015b (The MathWorks Inc., Natick, MA, 2015), the effect of muscle configuration (Weak TA and Weak EDL) and injuries (ΔATFL and ΔATFL-CFL) compared to baseline (intact ankle with physiological load set) on the measured ankle joint kinematics was determined using a repeated measures analysis of variance (ANOVA) on the dependent variables of measured rotation and translation at twenty-percent increments of dorsiflexion/plantarflexion.

5.3. Results

5.3.1. Biomechanics of Muscle Contributions

For physiological load set, the inversion increased in dorsiflexion, but then decreased throughout the cycle (Figure 5.2). Different muscle loading configurations displayed opposing effects on the kinematics significantly ($p<0.001$). The Weak EDL increased the inversion from 1.9° to 3.8°, while the Weak TA resulted in a significantly lower inversion throughout the flexion. Internal rotation in the physiological set increased to a maximum from fully dorsiflexion to the early plantarflexion, and then decreased (Figure 5.3). More external rotation in the Weak TA and more internal rotation in the Weak EDL with respect to the physiological load set throughout the full cycle were observed ($p<0.0005$). In medial-lateral translation, Weak EDL shows a decrease in medial translation; however, Weak TA demonstrates a significant increase in average medial translation of 1.5 mm ($p<0.01$) (Figure 5.4). When the TA muscle was less loaded, AJC moved posteriorly throughout the cycle, while when the EDL had less loads than TA the AJC moved posteriorly in dorsiflexion and anteriorly in plantarflexion ($p<0.001$) (Figure 5.5). No displacement was seen in inferior-superior in dorsiflexion for physiological set, although the ankle moved superiorly in plantarflexion (Figure 5.6). Inferior-superior translation was not significantly different with different muscle strengths ($p>0.05$). Reduced loads on the TA and EDL resulted in a significant change in the Achilles tendon only for dorsiflexion ($p<0.005$) not the plantar flexion ($p>0.05$) (Figure 5.7).

5.3.2. Biomechanics of Injury

For the intact ankle, inversion increased until early dorsiflexion and then decreased for the rest of the cycle (Figure 5.8). The injuries did change the inversion significantly in the early dorsiflexion ($p<0.05$); however, the inversion was not different significantly and only a trend was

seen the rest of the cycle ($p<0.1$). Internal rotation was increased from the intact ankle up to mid-plantarflexion and after that decreased approximately 2 degrees (Figure 5.9). Grade II and Grade III injury increased the internal rotation but not significantly ($p>0.05$). Throughout the cycle the calcaneus moved laterally, although this lateral movement increased until mid-flexion and then decreased to the fully plantarflexed ankle (Figure 5.10). Grade III injury moved the AJC to the lateral side throughout the cycle, but ANOVA did not show a significant difference ($p>0.05$). The AJC moved from posterior position to anterior position in the intact ankle during the cycle for reasons discussed previously (Figure 5.11). An increase in anterior movement was seen significantly for Grade II and Grade III injury in the dorsiflexion ($p<0.05$), although it did not reach significance in plantarflexion ($p>0.05$). Superior-inferior translation was not significantly different due to the injury ($p>0.05$) (Figure 5.12). Achilles load increased over the cycle for the intact ankle (Figure 5.13). A significant increase in the load difference was seen for both injuries in deep plantarflexion ($p<0.01$), while the increase in the loads were not significant in the rest of the cycle ($p>0.05$).

5.4. Discussion

5.4.1. Biomechanics of Muscle Contributions

In this study the ankle joint complex kinematics of both the Weak TA and the Weak EDL loading configurations deviated from the physiological one. The study determined that changes in the loading configurations of the TA and EDL muscles affect the ankle inversion and internal rotation throughout the flexion range. Resultant kinematic behavior was similar to a study by Siegler, 1988 (Siegler et al., 1988); however, the inversion in this study was considerably higher since the tibialis anterior was loaded. Additionally, in this study, the ankle joint complex was

shown internally rotated in the physiological loading set because the TA has a greater role in internal rotation and the EDL is not strong enough to prevent the internal rotation.

Inversion increased significantly and became greater during flexion when the TA was loaded less and the EDL was loaded more, which supports the observation that the EDL is the main evertor in the ankle. Subsequently, when there was a higher load on the TA and lower load on the EDL, more inversion was observed. The EDL weakness resulted in higher TA loads in the specimens, which suggested that patients could be more susceptible to hyper-inversion injuries. Thus, patients might not be able to achieve their normal range of motion in inversion. Strengthening the EDL can help stabilize the joint by reducing any excessive inversion.

Both muscle loading configurations resulted in similar behavior in internal-external and inversion-eversion rotations. This demonstrated that a coupling is happening with inversion-internal rotation of the AJC and eversion-external rotation of the AJC. Moreover, this study reveals that the variation in muscle contribution does not change the extent of coupling during the flexion and extension by showing similar total changes.

The higher medial and posterior translation of the AJC while the TA had less load on it demonstrated that the tibialis anterior is stabilizing the AJC not only laterally but also anteriorly. However, the weaker EDL stabilize the AJC only posteriorly. Thus, by strengthening the TA, patients are able to achieve a better stabilization in their AJC. Lack of significance in superior-inferior change shows that TA and EDL muscles are not contributing in this motion for the AJC considerably.

The total static loads on the muscles were constant in different muscle contribution for better demonstration of the impacts of the TA and EDL contribution in the Achilles load. Based on the constant total load, the first hypothesis was that the Achilles load stays constant during the

cycle. However, the Achilles experienced higher loads during flexion when the TA had larger loads on it, and less loads during late flexion when the TA had smaller loads. This indicates that the EDL contributes less in dorsiflexion than the TA. However, less load on the TA or higher load on the EDL only decreased the Achilles load generation in the late dorsiflexion which demonstrates that the TA and EDL have more contribution in dorsiflexion and Achilles has the most contribution in the plantarflexion not dorsiflexion.

5.4.2. Biomechanics of Injury

The objectives of this study were to develop a better understanding of the kinematic changes that occur in response to Grade III sprains of the ATFL and CFL under muscle loaded conditions. Similar overall ranges of motion were observed in the intact ankles as had previously been reported (Siegler et al., 1988).

ATFL rupture was hypothesized to result in changes to anterior translation and inversion in deep plantarflexion due to its orientation in the anterior direction and the relative motion of the talus and fibula. There was a slight increase to inversion in the trials as the ankle became more plantarflexed similar to Bahr et al. (Bahr et al., 1998), although it did not reach significance. The maximum strain of the ATFL occurs in plantarflexion and supination, which is a combination of inversion and internal rotations (Bahr et al., 1998; de Asla et al., 2009). Under muscle-loaded conditions, the data do not show any significant difference in anterior-posterior translation. This was unexpected because previous work had shown that increased compression at the joint increased load in the ATFL (Bahr et al., 1998). It is possible that the additional moments and forces applied by the muscles act to increase constraint of the joint thereby shielding the effects of ATFL rupture.

The CFL is typically noted to have increased load and elongation, specifically in dorsiflexion and either pronation (de Asla et al., 2009) or supination (Bahr et al., 1998). The slanted posterior, distal direction of the ligament suggests that the CFL would resist external rotation as well as inversion of the ankle, and it was hypothesized that the combined ATFL-CFL rupture would result in a reduction of constraint in these motions. After the simulated Grade III CFL injury, the trials demonstrated significant changes to inversion, internal rotation, and anterior translation similar to what has been previously reported in literature (Petersen et al., 2013). A rotation of the ligament's orientation during flexion may explain this dual role in anterior-posterior motion. Similarly, the CFL has a role in both internal and external constraint. The CFL therefore is a major contributor to AJC constraint in the transverse plane. Previous literature reported the greatest reduction of constraint following CFL damage to occur in either dorsiflexion (Hollis et al., 1995) or plantarflexion (Johnson and Markolf, 1983) whereas it appears to be reduced uniformly throughout flexion in this study. This indicates that a damaged or weaker ATFL would be a predictor of future CFL injury. Stabilizing the ankle joint throughout recovery is crucial to preventing further damage.

The muscle-loaded data revealed that there likely is greater variability in the ATFL and CFL. The standard deviation of the change after ATFL injury is considerably higher relative to that of the combined rupture. While the additional CFL rupture displayed more similar changes to constraint, it is probable that, independent of the ATFL tear, CFL-rupture would display similar standard deviations. Once both ligaments are ruptured and constraint depends more on geometric interactions and the remaining soft tissue, the variability drops indicating these parameters play a more constant role between specimens.

Patients often feel pain and earlier exhaustion after sprains (de Asla et al., 2009). Both injury conditions increased the Achilles load necessary to flex the ankle, but only the combined ATFL-CFL rupture reached significance. The magnitudes of the loads applying a dorsiflexion moment are constant throughout all trials, so a change in the moment arms of the muscles due to injury is likely the cause. Anterior translation of the calcaneus would increase the moment arms of the TA and EDL while decreasing the moment arm of the Achilles tendon resulting in higher load through the gastrocnemius and soleus. The increase in Achilles load can explain the patients' exhaustion, and should be considered in the physical therapy training that is assigned to the patients after injury.

Both ligaments displayed significant effects on the Achilles load. The Achilles has to generate more loads to stable the ankle during early flexion angles after the injury, and the difference decreases with flexion. The decrease in the ankle load can be explained by Achilles' fascicle length drops in the plantarflexion. The shorter fascicle length results in the lower force generation of the Achilles tendon. Other studies displayed that patients feel pain and sooner tiredness according to the CFL injury.

5.5. Conclusion

This study revealed the contribution of tibialis anterior and extensor digitorum longus muscles as well as the influence of the injury on the biomechanics of the ankle joint complex. Outcomes suggest that the tendons are not affecting the coupling between internal and inversion rotations, and the higher loads in the Achilles tendon after the injury shows that the physical therapists can target the gastrocnemius and solenous muscles in the sessions of rehabilitation for patients to reduce their pain in daily activities. Results may affect prescribed rehabilitation of the

ankle, help to verify computational models, and improve our understanding of ankle injury and collateral ligaments' functions.

There are a few limitations to this study. First, a small study size was used (n = 9). Additional studies should be performed to determine if the trends and significant differences accurately represent the total population. The muscle loads used were relatively small compared to the physiological loads in the body, so the results from that data may not reflect the effect of injury during daily activities. Furthermore, no ground reaction forces were examined, and the tests did not account for variation in muscle activity throughout flexion. Tendons exhibit hysteresis during repetitively motions; however, in this study the hysteresis effects diminished by setting up the experiment after a laxity experiment.

In this study, our objective was to quantify the AJC biomechanics, yet understanding the effect of injury on the subtalar and talocrural joints is also important and should be considered in future research. Simulation of injuries was done by completely rupturing the ligaments, which is the worst case of injury and is not reflective of the partial ruptures that occur in many sprains. The CFL sprain was compounded onto the ATFL sprain because damage rarely occurs solely to the CFL, but studying isolated CFL rupture would provide additional information about the ligament's role in an intact ankle. Future research is needed to understand various ruptures.

Table 5.1. The TA and EDL load magnitudes for the three loading sets

Configuration	TA (N)	EDL (N)
Physiological	90	45
Weak TA and Strong EDL (ΔL2)	67.5	67.5
Weak EDL and Strong TA (ΔL3)	112.5	22.5

Table 5.2. Ranges of motion of ankle specimen. Anterior-Posterior translation excluded due to large dependence on flexion angle.

Motion	Range of Motion (ROM)	
	Mean ± STD	**Range**
Plantarflexion	46.7° ± 7.8°	36.0° to 61.7°
Dorsiflexion	32.3° ± 6.3°.	22.0° to 41.8°
Inversion	17.9° ± 3.9°.	12.1° to 23.7
Eversion	10.3° ± 2.8°.	4.8° to 13.6°
Internal Rotation	23.3° ± 6.0°	15.1° to 21.6°
External Rotation	13.9° ± 3.9°.	7.2° to 19.2°

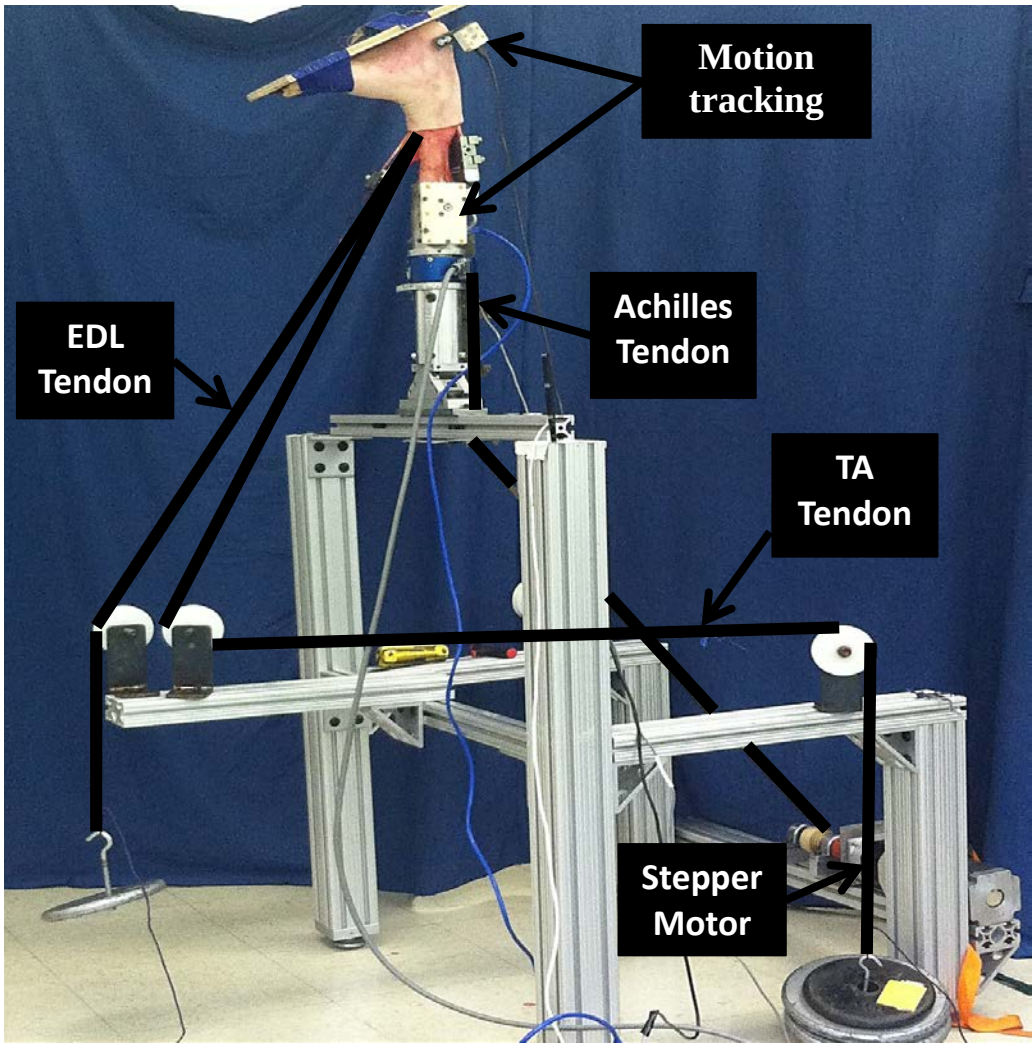

Figure 5.1. Experimental setup: the tibia is potted into an aluminum fixture and tendons are loaded with static weights and a stepper motor.

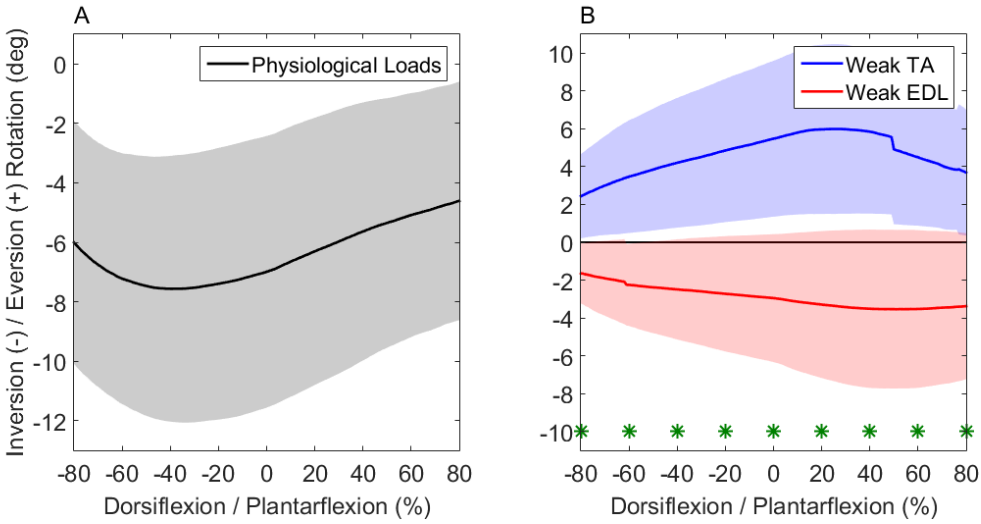

Figure 5.2. (A) Inversion-eversion in physiologically loaded set. (B) Inversion-eversion change for different trials. Statistical significant differences (p < .05) are shown by (*). The shaded area represents data within ±1 standard deviation

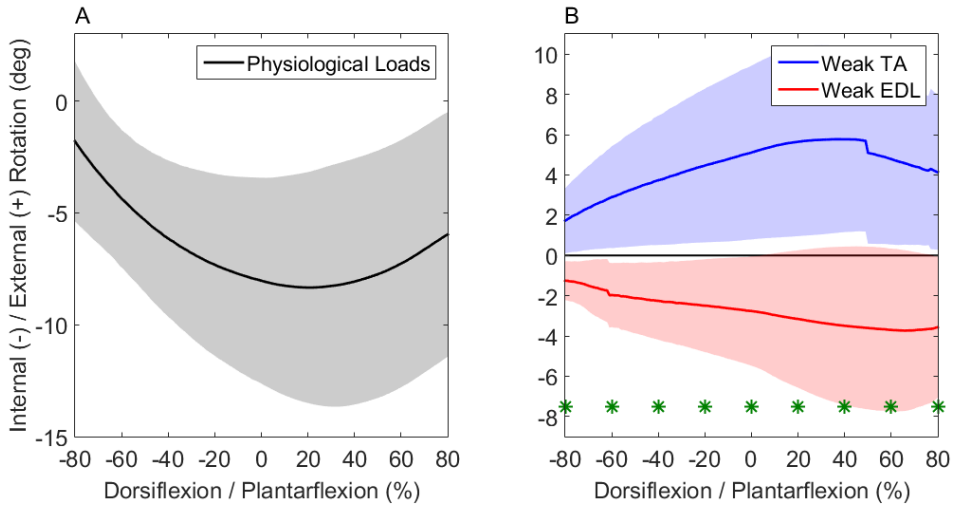

Figure 5.3. (A) Internal-external in physiologically loaded set. (B) Internal-external change for different trials. Statistical significant differences (p < .05) are shown by (*). The shaded area represents data within ±1 standard deviation

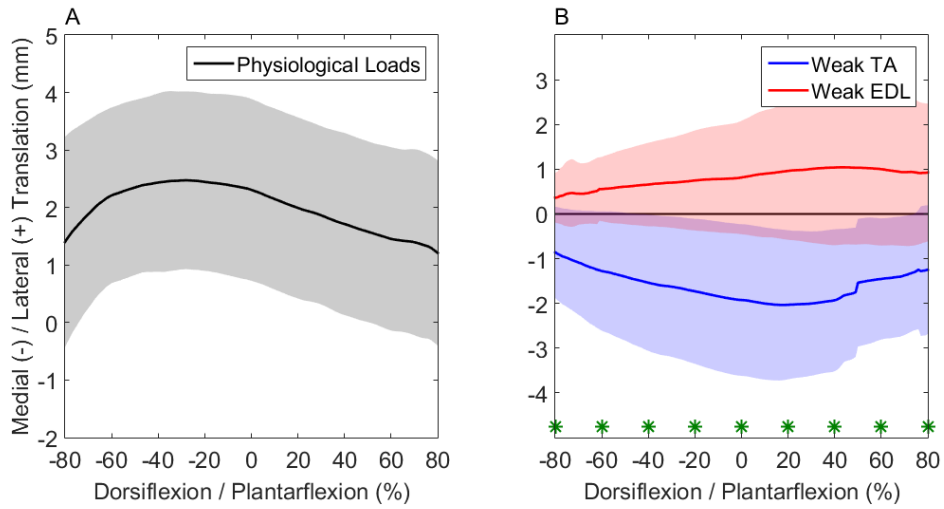

Figure 5.4. (A) Medial-lateral translation in physiologically loaded set. (B) Medial-lateral change for different trials. Statistical significant differences (p < .05) are shown by (*). The shaded area represents data within ±1 standard deviation

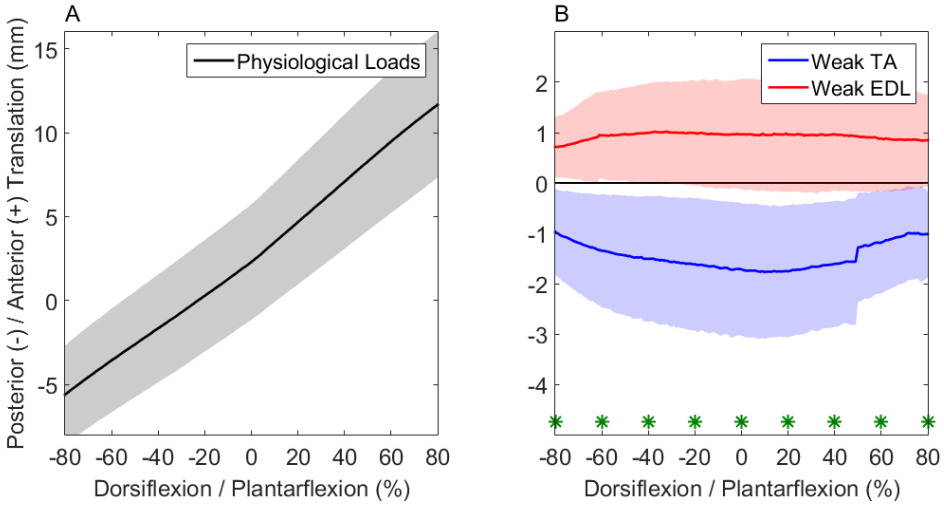

Figure 5.5. (A) Posterior-anterior translation in physiologically loaded set. (B) Posterior-anterior change for different trials. Statistical significant differences (p < .05) are shown by (*). The shaded area represents data within ±1 standard deviation

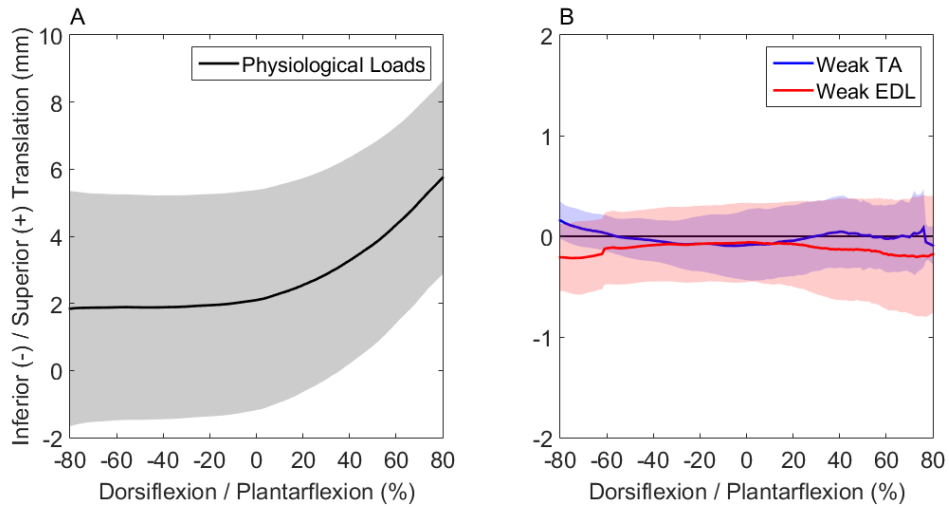

Figure 5.6. (A) Inferior-superior translation in physiologically loaded set. (B) Inferior-superior change for different trials. No statistical significant differences ($p < .05$) were seen. The shaded area represents data within ±1 standard deviation

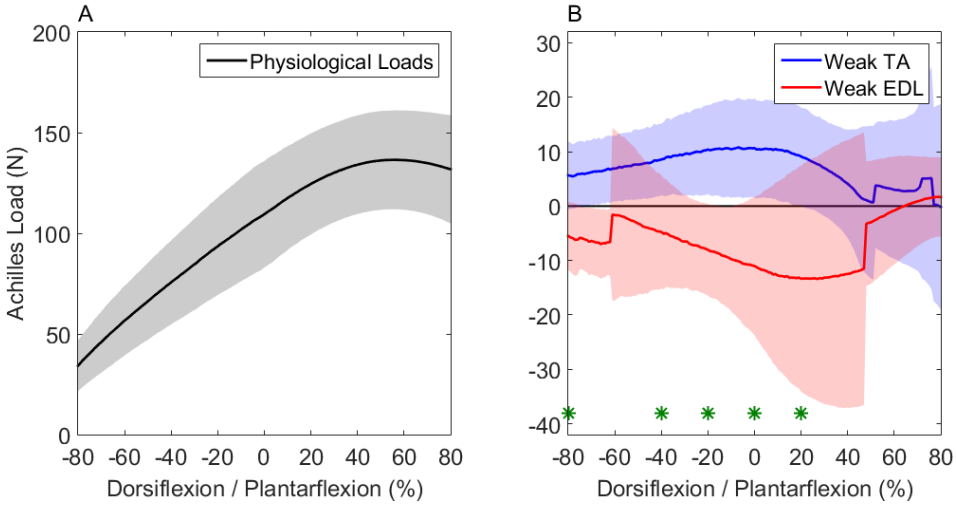

Figure 5.7. (A) Achilles load while the muscles were loaded physiologically. (B) Achilles load for different trials. Statistical significant differences ($p < .05$) are shown by (*). The shaded area represents data within ±1 standard deviation

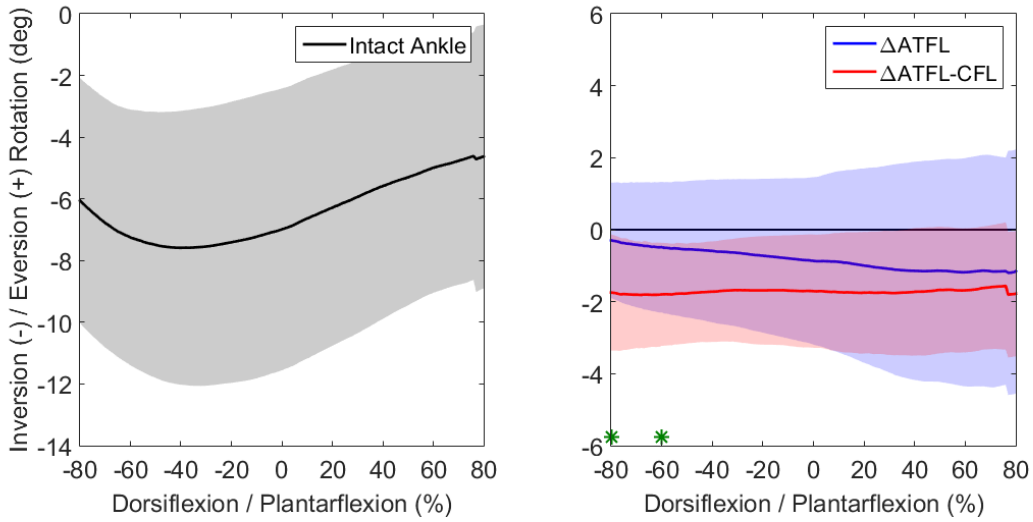

Figure 5.8. Inversion-eversion rotation during muscle-loaded kinematic trials. Statistical significant differences ($p < .05$) are shown by (*). The shaded area represents data within ±1 standard deviation

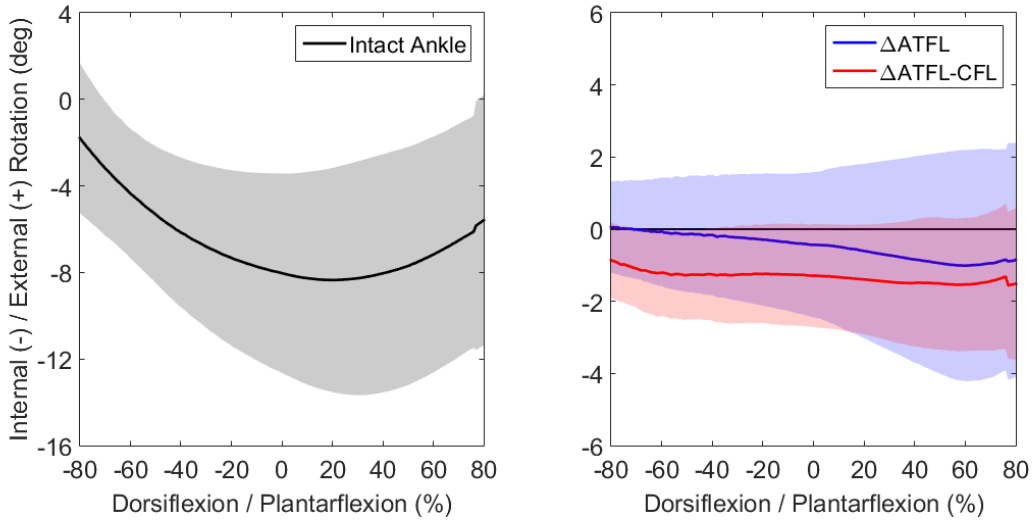

Figure 5.9. Internal-external rotation during muscle-loaded kinematic trials. No statistical significant differences ($p < .05$) were seen. The shaded area represents data within ±1 standard deviation

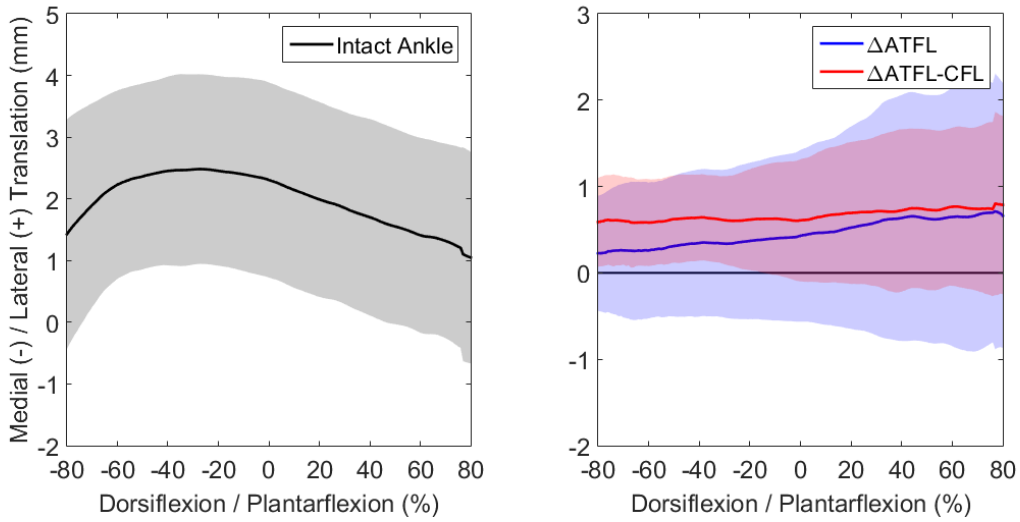

Figure 5.10. Medial-lateral translation during muscle-loaded kinematic trials. No statistical significant differences ($p < .05$) were seen. The shaded area represents data within ±1 standard deviation

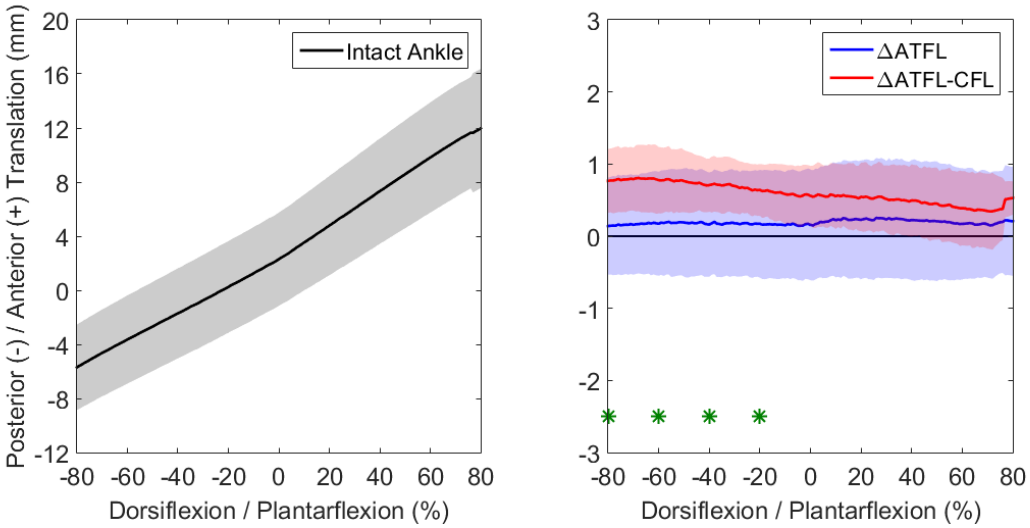

Figure 5.11. Posterior-anterior translation during muscle-loaded kinematic trials. Statistical significant differences ($p < .05$) are shown by (*). The shaded area represents data within ±1 standard deviation

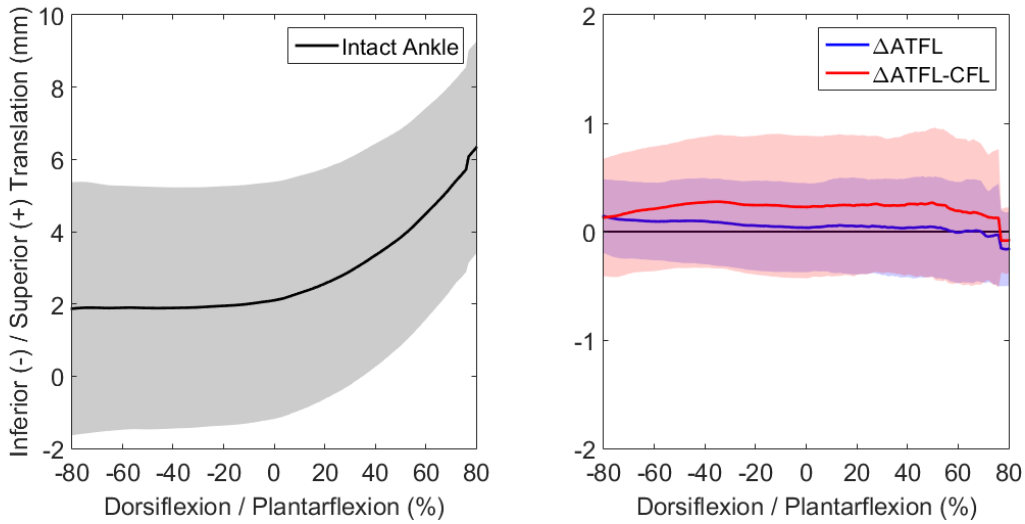

Figure 5.12. Inferior-superior translation during muscle-loaded kinematic trials. No statistical significant differences ($p < .05$) were seen. The shaded area represents data within ±1 standard deviation

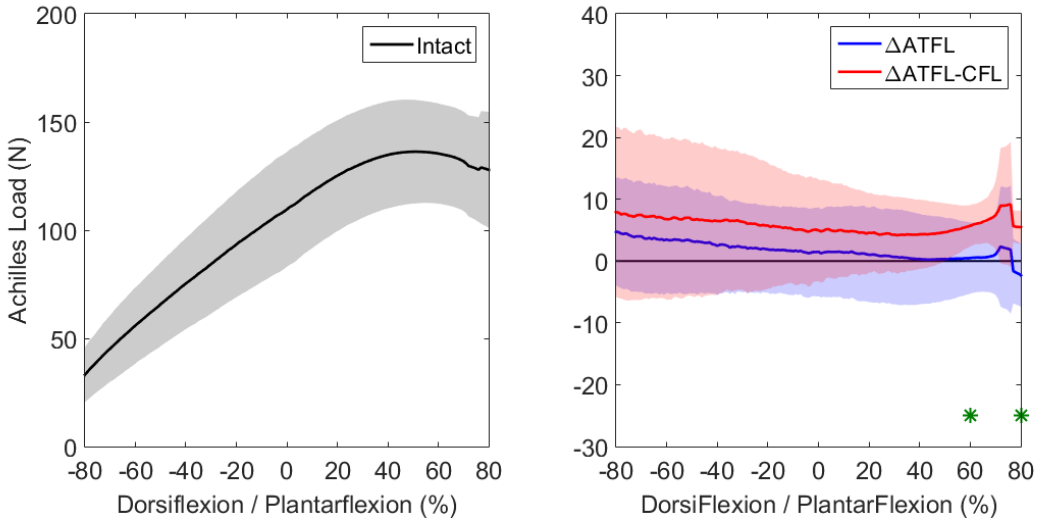

Figure 5.13. Achilles load during muscle-loaded kinematic trials. Statistical significant differences ($p < .05$) are shown by (*). The shaded area represents data within ±1 standard deviation

6. Conclusion and Future Work

Observing a high rate of injuries per athlete-exposures, this research was focused on the subject and tried to improve understanding of the injuries with the goal of preventing them or enhancing rehabilitation. The first aim was designing a machine for simulating the helmet collisions and evaluate the influence of the neck stiffness on the head and helmet acceleration after the impact, and the second aim was characterizing the collateral ligament injuries in an *in-vitro* model of the ankle joint and analyze the muscle contribution to it.

To study the first objective, a machine for replicating the helmet collisions in the field was designed and built. The computational model of the machine, before construction of it, helped with modifying the design and designing the experiment. Testing different stiffness levels, the simulated collisions demonstrated that the neck stiffness does not change the peak helmet acceleration significantly. It was quantified and demonstrated that the helmets are reducing the head acceleration and increasing the rise time for the maximum head acceleration significantly which shows the great contribution of helmets in reduction of concussion. Since this study was mainly designing and creating the tool for experiment, it needs some additional steps in the future. Adding a customized damper to the neck can modify the neck mechanics. In this study, only one helmet was used from Schutt Inc.; however, different helmets could be put on the dummy to test the padding differences on the reduction of the head peak acceleration. Simulating different impact locations, different line of actions for springs, or even simulating different frictions on the sled, could show interesting results in the future. Moreover, if a new design of helmet or shoulder pads come up, the machine is able to validate and investigate the advantages or disadvantages of that. Moreover, the computational model can be validated to study objectives that are hard to achieve

in the machine like side impacts, dampening of the neck, pendulum weight variations to look at the impact of the head velocity, and other studies could be run.

The study of the second aim revealed the contribution of tibialis anterior and extensor digitorum longus muscles as well as the influence of the injury on the biomechanics of the ankle joint complex. Outcomes suggest that the tendons are not affecting the coupling between internal and inversion rotations. The higher loads in Achilles after the injury shows that the physical therapists can target the Achilles tendon in the sessions of rehabilitation for patients to reduce their pain in daily activities. Results may affect prescribed rehabilitation of the ankle, help to verify computational models, and improve our understanding of ankle injury and collateral ligaments' functions. In this study, our objective was to quantify the AJC biomechanics, yet understanding the effect of injury on the subtalar and talocrural joints is also important and should be considered in future research. Simulation of injuries was done by completely rupturing the ligaments, which is the worst case of injury and is not reflective of the partial ruptures that occur in many sprains. The CFL sprain was compounded onto the ATFL sprain because damage rarely occurs solely to the CFL, but studying isolated CFL rupture would provide additional information about the ligament's role in an intact ankle. Future research is needed to understand various ruptures. The fifth chapter of this document was published as two conference abstracts in 2015 at SB^3C, Utah (Appendix C and D).

References

AnatomyCharts, 2016. Human Calf Muscles Anatomy. Digital image. Web 14 Jul 2016. <http://anatomycharts.us/wp-content/uploads/2015/11/human-calf-muscles-anatomy-bodyman-matrix-of-calf-muscles-summery.jpg>.

Arnold, E.M., Ward, S.R., Lieber, R.L., Delp, S.L., 2010. A model of the lower limb for analysis of human movement. Annals of biomedical engineering 38, 269-279.

Bahr, R., Pena, F., Shine, J., Lew, W.D., Engebretsen, L., 1998. Ligament force and joint motion in the intact ankle: a cadaveric study. Knee surgery, sports traumatology, arthroscopy : official journal of the ESSKA 6, 115-121.

Bartsch, A., Benzel, E., Miele, V., Morr, D., Prakash, V., 2012a. Hybrid III anthropomorphic test device (ATD) response to head impacts and potential implications for athletic headgear testing. Accident Anal Prev 48, 285-291.

Bartsch, A., Benzel, E., Miele, V., Prakash, V., 2012b. Impact test comparisons of 20th and 21st century American football helmets. Journal of neurosurgery 116, 222-233.

Beckman, S.M., Buchanan, T.S., 1995. Ankle Inversion Injury and Hypermobility - Effect on Hip and Ankle Muscle Electromyography Onset Latency. Arch Phys Med Rehab 76, 1138-1143.

Brooks, S.C., Potter, B.T., Rainey, J.B., 1981. Treatment for partial tears of the lateral ligament of the ankle: a prospective trial. British medical journal 282, 606-607.

Brostroem, L., 1964. Sprained Ankles. I. Anatomic Lesions in Recent Sprains. Acta chirurgica Scandinavica 128, 483-495.

Burks, R.T., Morgan, J., 1994. Anatomy of the lateral ankle ligaments. The American journal of sports medicine 22, 72-77.

Crisco, J.J., Greenwald, R.M., 2011. Let's get the head further out of the game: a proposal for reducing brain injuries in helmeted contact sports. Current sports medicine reports 10, 7-9.

de Asla, R.J., Kozanek, M., Wan, L., Rubash, H.E., Li, G., 2009. Function of anterior talofibular and calcaneofibular ligaments during in-vivo motion of the ankle joint complex. Journal of orthopaedic surgery and research 4, 7.

Devries, J.G., Berlet, G.C., Lee, T.H., Hyer, C.F., Deorio, J.K., 2011. Revision total ankle replacement: an early look at agility to INBONE. Foot & ankle specialist 4, 235-244.

DocPods, 2016. Ankle Sprain. Digital image. Web 14 Jul 2016. <http://www.docpods.com/ankle-sprains>.

Engebretsen, A.H., Myklebust, G., Holme, I., Engebretsen, L., Bahr, R., 2010. Intrinsic risk factors for acute ankle injuries among male soccer players: a prospective cohort study. Scandinavian journal of medicine & science in sports 20, 403-410.

Funk, J.R., Cormier, J.M., Bain, C.E., Guzman, H., Bonugli, E., 2009. Validation and Application of a Methodology to Calculate Head Accelerations and Neck Loading in Soccer Ball Impacts. Society of Automotive Engineers, Warrendale, Penn.

Gallo, R.A., Kolman, B.H., Daffner, R.H., Sciulli, R.L., Roberts, C.C., DeMeo, P.J., 2004. MRI of tibialis anterior tendon rupture. Skeletal radiology 33, 102-106.

Gerbeding, J., 2003. Report to Congress on Mild Traumatic Brain Injury in the United States: Steps to Preventing a Serious Public Health Problem. Center for Disease Control and Prevention, Atlanta (GA), pp. 1-5.

Grood, E.S., Suntay, W.J., 1983. A joint coordinate system for the clinical description of three-dimensional motions: application to the knee. Journal of biomechanical engineering 105, 136-144.

Gwin, J.T., Chu, J.J., Diamond, S.G., Halstead, P.D., Crisco, J.J., Greenwald, R.M., 2010a. An Investigation of the NOCSAE Linear Impactor Test Method Based on In Vivo Measures of Head Impact Acceleration in American Football. J Biomech Eng-T Asme 132.

Gwin, J.T., Chu, J.J., Diamond, S.G., Halstead, P.D., Crisco, J.J., Greenwald, R.M., 2010b. An investigation of the NOCSAE linear impactor test method based on in vivo measures of head impact acceleration in American football. Journal of biomechanical engineering 132, 011006.

Hernandez, F., Shull, P.B., Camarillo, D.B., 2015. Evaluation of a laboratory model of human head impact biomechanics. Journal of biomechanics 48, 3469-3477.

Hertel, J., 2002. Functional Anatomy, Pathomechanics, and Pathophysiology of Lateral Ankle Instability. Journal of athletic training 37, 364-375.

Hollis, J.M., Blasier, R.D., Flahiff, C.M., 1995. Simulated lateral ankle ligamentous injury. Change in ankle stability. The American journal of sports medicine 23, 672-677.

Johnson, E.E., Markolf, K.L., 1983. The contribution of the anterior talofibular ligament to ankle laxity. The Journal of bone and joint surgery. American volume 65, 81-88.
Johnston, J.M., Ning, H., Kim, J.-E., Kim, Y.-H., Soni, B., Reynolds, R., Cooper, L., Andrews, J.B., Vaidya, U., 2015. Simulation, fabrication and impact testing of a novel football helmet padding system that decreases rotational acceleration. Sports Engineering 18, 11-20.
Kidport, 2016. Ankle Joint and Bones. Digital image. Web 14 Jul 2016 <http://www.kidport.com/reflib/science/humanbody/skeletalsystem/Ankle.htm>.
King, A.I., Yang, K.H., Zhang, L., Hardy, W., Viano, D.C., Year Is head injury caused by linear or angular acceleration. In IRCOBI conference.
Kleiven, S., 2013. Why most traumatic brain injuries are not caused by linear acceleration but skull fractures are. Frontiers in Bioengineering and Biotechnology 1.
Langlois, J.A., Rutland-Brown, W., Wald, M.M., 2006. The epidemiology and impact of traumatic brain injury: a brief overview. The Journal of head trauma rehabilitation 21, 375-378.
Lewis, L.M., Naunheim, R., Standeven, J., Lauryssen, C., Richter, C., Jeffords, B., 2001. Do Football Helmets Reduce Acceleration of Impact in Blunt Head Injuries? Academic Emergency Medicine 8, 604-609.
Linder, A., Svensson, M.Y., Davidsson, J., Flogård, A., Håland, Y., Jakobsson, L., Lövsund, P., Wiklund, K., 1998. The New Neck Design for the Rear-End Impact Dummy, BioRID I. Annual Proceedings / Association for the Advancement of Automotive Medicine 42, 179-192.
Louisvilleorthopedics, 2016. Ankle Sprain. Digital image. Web 14 Jul 2016 <http://louisvilleorthopedics.com/library/patient-education/sprained-ankle/>.
McKay, G.D., Goldie, P.A., Payne, W.R., Oakes, B.W., 2001. Ankle injuries in basketball: injury rate and risk factors. British journal of sports medicine 35, 103-108.
Meriam, J.L., Kraige, L.G., 2012. Engineering mechanics, 7th ed. J. Wiley, New York.
Mertz, H.J., Patrick, L.M., 1971. Strength and Response of the Human Neck*. SAE International.
Mizel, M.S., Hecht, P.J., Marymont, J.V., Temple, H.T., 2004. Evaluation and treatment of chronic ankle pain. Instructional course lectures 53, 311-321.
Murphy, R.A., 1983. Basic Human Anatomy - a Regional Study of Human Structure - Orahilly,R. New Engl J Med 309, 248-248.

Newman, J.A., Shewchenko, N., Welbourne, E., 2000. A proposed new biomechanical head injury assessment function - the maximum power index. Stapp car crash journal 44, 215-247.
NOCSAE, 1998. Standard Drop Test Method and Equipment Used in Evaluating the Performance Characteristics of Protective Headgear. National Operating Committee on Standards for Athletic Equipment, Overland Park, KS.
NOCSAE, 2006. Standard Linear Impactor Test Method and Equipment Used in Evaluating the Performance Characteristics of Protective Headgear and Faceguards. National Operating Committee on Standards for Athletic Equipment, Overland Park, KS.
Payne, K.A., Berg, K., Latin, R.W., 1997. Ankle injuries and ankle strength, flexibility, and proprioception in college basketball players. Journal of athletic training 32, 221-225.
Pellman, E.J., Viano, D.C., Tucker, A.M., Casson, I.R., Committee on Mild Traumatic Brain Injury, N.F.L., 2003a. Concussion in professional football: location and direction of helmet impacts-Part 2. Neurosurgery 53, 1328-1340; discussion 1340-1321.
Pellman, E.J., Viano, D.C., Tucker, A.M., Casson, I.R., Waeckerle, J.F., 2003b. Concussion in professional football: reconstruction of game impacts and injuries. Neurosurgery 53, 799-812; discussion 812-794.
Pellman, E.J., Viano, D.C., Withnall, C., Shewchenko, N., Bir, C.A., Halstead, P.D., 2006. Concussion in professional football: helmet testing to assess impact performance--part 11. Neurosurgery 58, 78-96; discussion 78-96.
Petersen, W., Rembitzki, I.V., Koppenburg, A.G., Ellermann, A., Liebau, C., Bruggemann, G.P., Best, R., 2013. Treatment of acute ankle ligament injuries: a systematic review. Archives of orthopaedic and trauma surgery 133, 1129-1141.
Pointinger, H., Munk, P., Poeschl, G., 2003. Rupture of the Extensor Digitorum Longus Muscle. European Journal of Trauma 29, 161-163.
Rowson, S., Brolinson, G., Goforth, M., Dietter, D., Duma, S., 2009. Linear and angular head acceleration measurements in collegiate football. Journal of biomechanical engineering 131, 061016.

Rowson, S., Duma, S.M., 2013. Brain Injury Prediction: Assessing the Combined Probability of Concussion Using Linear and Rotational Head Acceleration. Annals of biomedical engineering 41, 873-882.
Siegler, S., Chen, J., Schneck, C.D., 1988. The three-dimensional kinematics and flexibility characteristics of the human ankle and subtalar joints--Part I: Kinematics. Journal of biomechanical engineering 110, 364-373.
Slimmon, D., Brukner, P., 2010. Sports ankle injuries Assessment and management. Aust Fam Physician 39, 18-22.
Spittle, E.K., Miller, D.J., Shipley Jr, B.W., Kaleps, I., 1992. Hybrid II and hybrid III dummy neck properties for computer modeling. DTIC Document.
Stahelin, A.C., Weiler, A., 1997. All-inside anterior cruciate ligament reconstruction using semitendinosus tendon and soft threaded biodegradable interference screw fixation. Arthroscopy : the journal of arthroscopic & related surgery : official publication of the Arthroscopy Association of North America and the International Arthroscopy Association 13, 773-779.
TheShockBox, 2016. DUMMYCLEAN. Digital image. Web 14 Jul 2016 <http://www.theshockbox.com/content/uploads/2012/12/dummyclean.jpg>.
Thurman, D.J., Branche, C.M., Sniezek, J.E., 1998. The epidemiology of sports-related traumatic brain injuries in the United States: recent developments. The Journal of head trauma rehabilitation 13, 1-8.
Viano, D.C., Withnall, C., Wonnacott, M., 2012. Football helmet drop tests on different fields using an instrumented Hybrid III head. Annals of biomedical engineering 40, 97-105.
Weindel, S., Schmidt, R., Rammelt, S., Claes, L., v Campe, A., Rein, S., 2010. Subtalar instability: a biomechanical cadaver study. Archives of orthopaedic and trauma surgery 130, 313-319.
Withnall, C., Bayne, T., 2004. Method and apparatus for testing football helmets. Google Patents.
Wu, G., Siegler, S., Allard, P., Kirtley, C., Leardini, A., Rosenbaum, D., Whittle, M., D'Lima, D.D., Cristofolini, L., Witte, H., Schmid, O., Stokes, I., Standardization, Terminology Committee of the International Society of, B., 2002. ISB recommendation on definitions of joint coordinate system

of various joints for the reporting of human joint motion--part I: ankle, hip, and spine. International Society of Biomechanics. Journal of biomechanics 35, 543-548.
Yoganandan, N., Pintar, F.A., Zhang, J.Y., Baisden, J.L., 2009. Physical properties of the human head: Mass, center of gravity and moment of inertia. Journal of biomechanics 42, 1177-1192.

Appendix A. Manual for MSC. Adams Model of the Impactor

The impactor computational models is consist of rigid bodies showing each machined parts in the system. Table A.1 lists the part name, their center of the mass location, and their mass used in the model. The head fixture considered as four parts, and the center of mass and the mass got calculated for the whole system. The units for locations are in inch. The 0, 0, 0 point is located for the easiness of drawing the cad model for the impactor.

A translational joint was considered between the sled and the rails without friction. A revolute joint was considered between the shaft of the arm and the arm. Another revolute joint was constructed for the neck, between the neck's plates. A torsional spring were positioned on the center of the plates with the spline deformation function as a stiffness. Three different elements were designed to show different level of stiffness, and were put in different sets based on the experiment. Other parts were attached to each other by fixed joints.

The contact was defined between a top neck plate and the plastic foam rubber on the lower neck plate. It was defined with a penalty of 10^9 with the restitution coefficient of 1.0. A solid to solid contact defined between the impactor head weight and the head. The normal force was designated as Impact with the stiffness of 4000, force exponent of 1.5, damping of 40.0, and the penetration depth of .00394 inches.

Table A.1. The impactor model rigid bodies center of mass location and mass

Part Name		Loc_X	Loc_Y	Loc_Z	Mass (kg)
Frame		-8.45	31.33	0	441.22
Pendulum		(LOC_RELATIVE_TO((45, 1.5, 1.5), Arm_Marker))			4.54
Weight_Base		(LOC_RELATIVE_TO((1.5, 3, 1.5), Weight_Strt_Pt))			(Pendulum_Weight)
Sled_Frame_Base		-19.11	4.2	0	26.3
Sled_Plae		-4.125	4.2	0	4.54
Torso		-7.0625	16.7	0	(Torso_Weight)
Spacer_Torso		-7.125	21.575	0	.46
Neck_Torso		-7.125	22.2	0	.91
Rubber		-7.125	22.5	0	.15
Head Fixture	Neck_Head	-7.125	22.8	0	0
	Spacer_Head	-7.125	23.425	0	0
	Head_Plate	(LOC_RELATIVE_TO((2.5, 0.25, 2.5), Head_Plate_M))			0
	Head_Head	(LOC_RELATIVE_TO((3, 4, 0), Center_ForJoint_M))			5.90
Helmet		-7.54	-30.02	0	.91

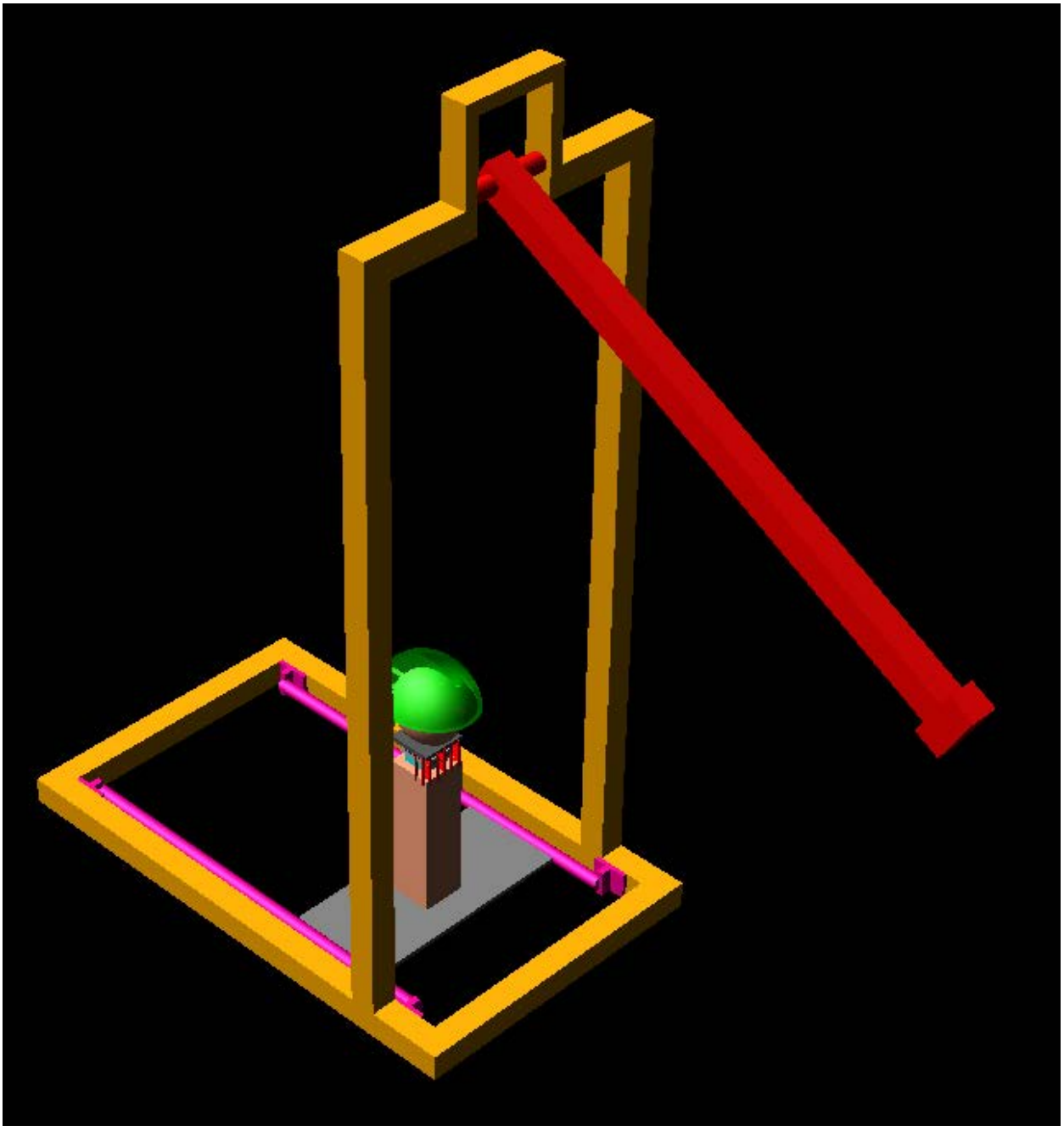

Figure A.1. The isometric view of the impactor computational model.

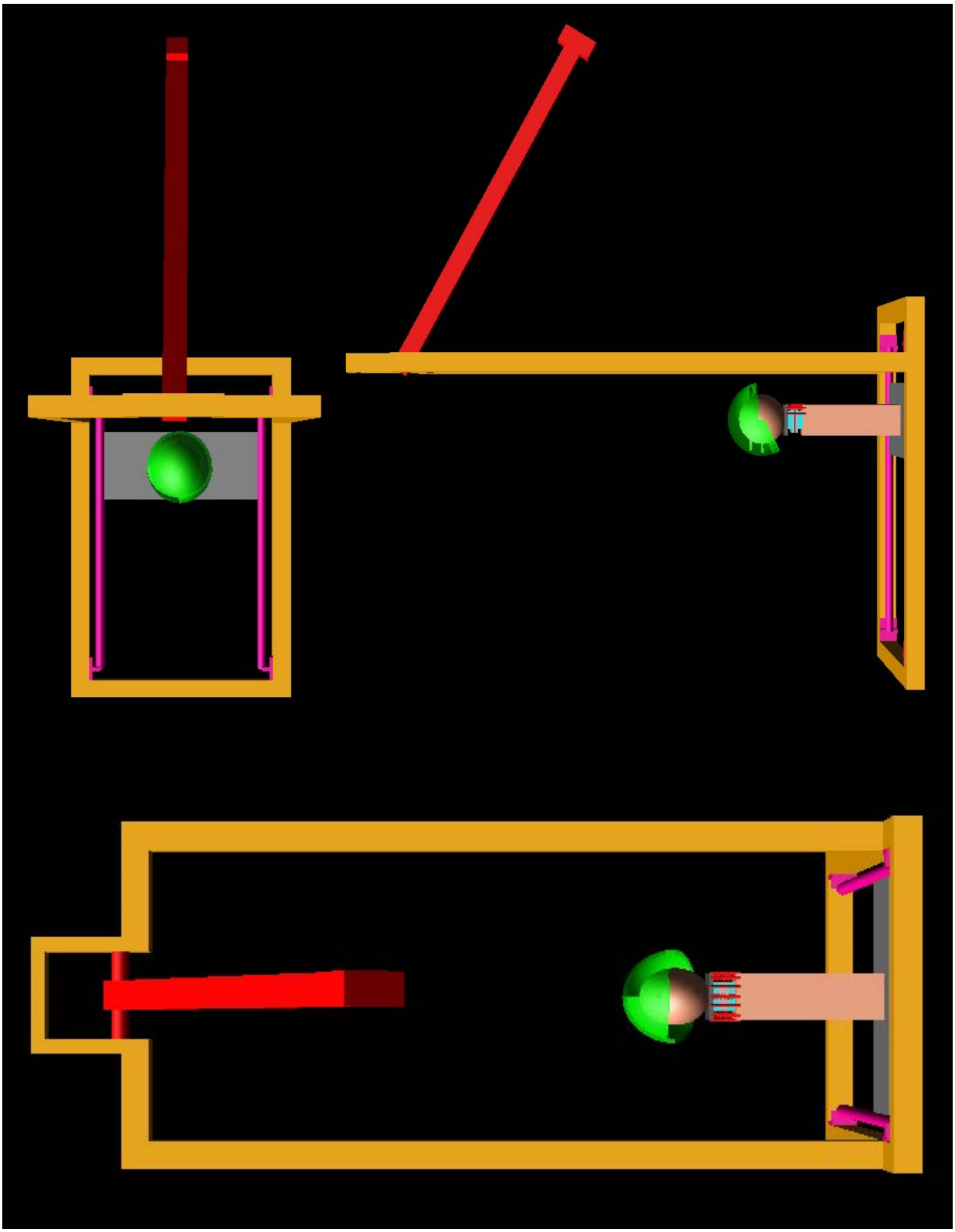

Figure A.2. The front, side, and the top view of the impactor computational model.

Appendix B. Computational model and designed study.

Table B.1. Computational model experiment. Springs were noted by K with N/mm unit. Dampers were noted by C with N.ms/mm unit

Exp.	Pendulum Weight (kg)	Release Angle (degree)	Neck Condition
#1	6.8	60◦	No Springs and Dampers
#2			K = 1.75
#3			K = 4.38
#4			K = 8.76
#5			Spring is Preloaded
#6			C = 175
#7			C = 876
#8			C = 1750
#10	9.0		C = 175
#11	11.4		C = 175
#12	6.8	30◦	C = 175
#13	6.8	45◦	C = 175

Table B.2. Designed Study. Pendulum head weight is 6.8 kg

Exp.	Impact Energy (Joules)	Neck Stiffness	Dropping Angle (degree)
#1	A	High	20°
#2		Medium	20°
#3		Low	20°
#4	B	High	40°
#5		Medium	40°
#6		Low	40°
#7	C	High	50°
#8		Medium	50°
#9		Low	50°
#10	D	High	60°
#11		Medium	60°
#12		Low	60°

Appendix C. Abstract 01, Podium Presentation at SB^{3}C, 2015

SB^{3}C2015
Summer Biomechanics, Bioengineering and Biotransport Conference
June 17-20, 2015,Snowbird Resort, Utah, USA
SB^{3}C2015-529

THE EFFECT OF GRADE II AND GRADE III ANKLE INJURY ON THE ANKLE JOINT COMPLEX KINEMATICS AND ACHILLES LOAD: A CADAVERIC STUDY

**Bardiya Akhbari (1), Matthew H. Dickinson (2), Ednah G. Louie (2) , Sami Shalhoub (2)
Lorin P. Maletsky (1, 2)**

(1) Department of Mechanical Engineering
University of Kansas
Lawrence, Kansas, United States

(2) Bioengineering Graduate Program
University of Kansas
Lawrence, Kansas, United States

INTRODUCTION

Inversion injuries of the ankle caused by rupture or sprain of collateral ligaments are very common and lead to deviations in joint stability.[1,2] *In-vivo* studies of ankle injuries are invasive due to a need to section the ligaments; hence *in-vitro* studies are preferred for understanding the variation in properties of injured and intact ankles. Previous in-vitro experiments studied the effects of ligaments sprain on the ankle joint complex kinematic without loading the muscles.[3] Understanding ankle joint complex (AJC) kinematics and kinetics allows for quantitative assessment of the talar tilt test and different mid-flexion assessments to be made in a total ankle replacement to create better outcomes for patients. The purpose of this study is to measure the effects of Grade II and Grade III ankle injury on the Achilles load, inversion/eversion, and adduction-/abduction of the AJC.

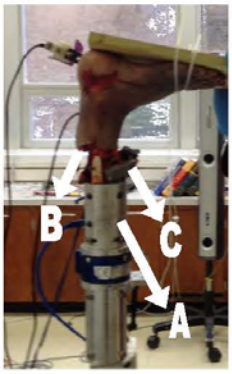

FIGURE 1: TESTING SETUP CONSISTING OF A) TIBIA FIXURE, B) MOTOR CABLE, C) MUSCLES CABLE

METHODS

Five fresh frozen cadaveric ankles were thawed at room temperature. The tibia was sectioned approximately 15cm superior to the calcaneus and potted in an aluminum fixture. The soft tissue above 15cm of the AJC joint line was removed except for the tibialis anterior (TA), extensor digitorum longus (EDL), and Achilles tendons, which were left intact. The ankle was then attached to a muscle-loading rig with the tibia rigidly fixed in an inverted position with the foot free to move (Figure 1). The TA and EDL and Achilles tendons were isolated and clamped individually. The ankle was flexed four times through its range of motion using a stepper motor attached to the Achilles tendon. Static loads were used to load the TA and the EDL. The physiological loading set was defined as 90N on the TA and 45N on the EDL based on their physiological cross sectional areas (PCSAs)[4]. Following literature,[5] a Grade II injury was simulated by resecting the anterior talofibular ligament (ATFL) followed by a resection of calcaneofibular ligament (CFL) to simulate a Grade III injury. After simulation of the injury and dissection of the ligaments, the skin and muscle were sutured to restrict excess movement of the ankle joint complex. The intact ankle experiment was used as the baseline kinematics and kinetics cycle during analysis.

The kinematics of the tibia and calcaneus were recorded using IRED markers rigidly attached to the bone and an Optotrak Certus motion-capture system (Northern Digital, Ontario). The loads applied by the motor on the Achilles tendon to dorsiflex/plantarflex the ankle were measured using a 1200N load cell (transducer technique). The difference in inversion/eversion (InEv), adduction/abduction (AdAb) rotation, and motor load (Load) were calculated for the two loading profiles relative to the baseline for the third motor's cycle. T-tests were performed to find significant differences ($p<0.05$) between the physiological configuration and each of the injured set individually.

RESULTS

The average kinematics for the five ankles displayed significant increase in inversion throughout the whole flexion cycle regardless of their injured or uninjured state (Figure 2.A). The average AdAb

rotation for the physiological load demonstrated changes in the abduction angle from approximately 4° to 5.3° of adduction during the whole cycle (Figure 2.C). The physiological load exhibited an increase in average Achilles load during early flexion and a decrease in the rest of the cycle (Figure 2.E). Moreover, increasing Achilles load was seen in early dorsiflexion, which decreased through the rest of the cycle. Both the Grade II and III injuries increased the inversion and Achilles' load throughout the entire cycle. Relative to the intact ankle, AdAb rotation remained the same for the Grade II injury and increased slightly in the Grade III injury during the entire cycle (Figure 2). The Grade II and III injuries resulted in an increase in ankle inversion throughout the cycle with an average of 0.8° and 1.6°, respectively (Figure 2.B). No change was seen in ankle adduction for the Grade II injury; however, with the Grade III injury the ankle was significantly more adducted than the intact ankle (Figure 2.D). The Achilles load was begun by 6.7N compensation and decreased during the entire cycle and finished by -0.4N. The load was more and significantly different for grade III which started from 11.6N and finished at 2.7N (Figure 2.F). The results displayed no statistical difference between the Grade II injured ankle and the intact ankle, nonetheless the Grade III injury presented a statistical difference of $p<0.05$ for inversion and the Achilles loads.

DISCUSSION

The effect of the collateral ligament rupture on the AJC kinematic was displayed by previous studies without additional muscles loads.[3] In this study the tibialis anterior and extensor digitorum longus muscles were loaded by physiological statics weight to exhibit the natural motion of AJC. The ankles inversion and adduction behavior during plantar flexion was similar to (Siegler, 1988) which studied the ankle three dimensional kinematics during natural motion without any loads attached to the muscles.[6] The inversion amount in this study was considerably higher which can be understood by the attached tibialis anterior static load. Moreover, Grade II and Grade III injuries were similar to what have been previously reported in the literature.[7]

Ruptures in the ATFL and CFL affect the ankle inversion at differing angles during the flexion range. In this study the AJC kinematics of both the injury Grade II and the injury Grade III deviated from the intact ankle, with the main variation observed in the inversion and loading. The higher inversion in the injuries was caused by absence of the collateral ligaments which have a main role in the rotation regulating of AJC. Rupture in the ATFL caused increase in the inversion difference during the whole cycle, while the rupture in both ligaments caused the decrease in the difference which verifies the fact that CFL has a large effect on the kinematic in the dorsiflexion.[5]

The insignificant dissimilarity in the AdAb motion in the Grade II injury and constant difference in this motion in Grade III injury displays the CFL role in stabilizing of ankle joint complex. In addition, ATFL role in the AdAb motion was minor which shows the minor change in AdAb follows by Grade II injury. Both ligaments displayed significant effects on the Achilles load. The Achilles has to generate more loads to stable the ankle during early flexion angles after the injury, and the difference decreases with flexion. The decrease in the ankle load can be explained by Achilles' fascicle length drops in the plantarflexion. The shorter fascicle length results in the lower force generation of the Achilles tendon. Other studies displayed that patients feel pain and sooner tiredness according to the CFL injury.[5]

The finding of this study has effect on the rehabilitation of the ankle movement, verifying the computational models, improving our understanding of the ankle injury and collateral ligaments function. There are a few limitations to this study; first the muscle loads used were relatively small compared to the physiological loads in the body. Low number of cadaveric specimen (five cadavers) was used and in order to improve the results, more specimens are needed. Simulation of injuries was to completely rupture the ligaments, which is the worst case of injury and is not reflective of partial ruptures in real-life sprains. Future research is needed to understand various ruptures. Moreover, variation in recognizing of the anatomical landmarks causes difference in the kinematic measurements for a single ankle; however the results for comparing between sets will not be changed.[8]

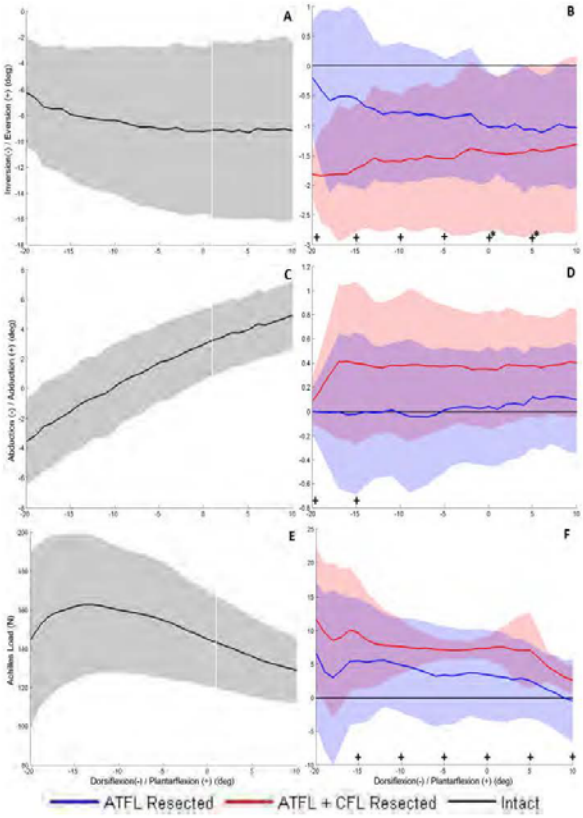

FIGURE 2: INEV (A), ADAB (C), AND LOAD (E) FOR ONE ANKLE, MEAN DIFFERENCE IN INEV (B), ADAB (D), AND LOAD (F) FOR ALL ANKLES BETWEEN PHYSIOLOGICAL AND INJURED SETS

(SIGNIFICANCE SHOWED BY * FOR GRADE II AND + FOR GRADE III INJURY)

ACKNOWLEDGEMENTS

This experiment was partially funded by DePuy Synthes, Inc.

REFERENCES

1.Brostroem L. Acta Chir Scand,128:483-95, 1964.
2.Brooks SC, et al. Br Med J (Clin Res Ed), 282(6264):606-7,1981.
3.West JE, University of Kansas. p 143 p, 2011.
4.Arnold EM, et al. Ann Biomed Eng,38(2):269-79, 2010.
5.de Asla RJ, et al. J Orthop Surg Res,4:7 , 2009.
6.Siegler S, et al.. J Biomech Eng, 110(4):364-73, 1988.
7.Petersen W, et al. Arch Orthop Trauma Surg, 133(8):1129-41, 2013.
8.Morton NA, et al. J of Orthop Research, 25(9):1221-1230, 2007.

Appendix D. Abstract 02, Poster Presentation at SB^{3}C, 2015

SB^{3}C2015
Summer Biomechanics, Bioengineering and Biotransport Conference
June 17-20, 2015,Snowbird Resort, Utah, USA
SB^{3}C2015-525

THE EFFECT OF MUSCLE LOADING ON ANKLE JOINT COMPLEX KINEMATICS AND ACHILLES LOAD: A CADAVERIC STUDY

Bardiya Akhbari (1), Matthew H. Dickinson (2), Ednah G. Louie (2) , Sami Shalhoub (2), Lorin P. Maletsky (1, 2)

(1) Department of Mechanical Engineering
University of Kansas
Lawrence, Kansas, United States

(2) Bioengineering Graduate Program
University of Kansas
Lawrence, Kansas, United States

INTRODUCTION

Injuries to the ankle joint are one of the most common sports injuries.[1] Inversion and adduction motion (together termed supination) injuries account for 80% of ankle's injuries.[2] Changes in the muscles' firing capability were seen after ankle sprain,[3] thus muscles activity in the gastrocnemius and soleus, tibialis anterior and extensor digitorum longus (antagonistic/agonistic muscles) will be changed after injury.[4]

Quantifying the effects of the tibialis anterior and extensor digitorum longus on the ankle joint complex will aid in muscle function analysis after injury by determining the effects of muscle weakness on the ankle joint kinematics. The purpose of this study was to measure the effects of variable tibialis anterior (TA) and extensor digitorum longus (EDL) muscle loading configurations on the ankle joint complex kinematics, and Achilles load.

METHODS

Five fresh frozen cadaveric ankles were thawed at room temperature. The tibia was sectioned 15 cm superior to the calcaneus and potted in aluminum fixtures. All soft tissue above 15 cm of the joint line was removed, except the TA, EDL, and Achilles tendon which were left intact. The ankle was then mounted onto an open chain muscle loading rig with the tibia rigidly attached in an inverted position and the foot free to move (Figure 1). The TA and EDL and Achilles tendons were isolated and clamped individually. The ankle was flexed four times over the entire range of flexion using a stepper motor attached to the Achilles tendon. Static loads were used to load the TA and the EDL. Three loading conditions were simulated: physiological loading defined as 90 N on the TA and 45 N on the EDL based on their physiological cross sectional area (PCSAs)[5], the second load set was defined as Weak EDL which reduced the EDL load from the physiological set to 50% , and the third load set defined as Weak TA which reduced the TA load from the physiological cycle to 75% of that (Table 1). Total static load on the tendons stayed 135 N during the load sets. The physiological load set was used as the baseline for comparison.

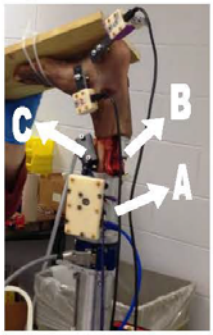

FIGURE 1: TESTING SETUP CONSISTING OF A) TIBIA FIXURE, B) MOTOR CABLE, C) MUSCLES CABLE

TABLE 1. TIBIALIS ANTERIOR AND EXTENSOR DIGITORUM LONGUS LOAD MAGNITUDES FOR THE THREE LOADING SETS

Configuration	TA	EDL
Physiological	90 N	45 N
Weak TA	67.5 N	67.5 N
Weak EDL	112.5 N	22.5 N

The kinematics of each bone were measured using IRED markers rigidly attached to the calcaneus and the tibia using an Optotrak Certus motion capture system (Northern Digital, Ontario). The loads applied by the motor onto the Achilles tendon to dorsiflex/plantarflex the ankle were measured using a 1200 N load cell (Transducer Technique, location). The difference in inversion/eversion (InEv), adduction-/abduction (AdAb) rotation, and Achilles load were calculated for the two loading cases relative to the baseline for the third motor's cycle in the -20° to 10° range of motion. A student t-tests was performed to find significant differences ($p<0.05$) between the physiological configuration and each of the two load sets individually.

RESULTS

The average kinematics of five ankles displayed significant increase in inversion throughout the whole flexion cycle (Figure 2.A). Different configuration displayed adverse effects on the ankles. The Weak EDL increased the inversion; however, the Weak TA resulted in significant and constant reduction (≈3°) in inversion (Figure 2.B). The maximum inversion difference for the Weak TA was 8.0°, although it was -3.3° for the Weak EDL. Investigation of average adduction/abduction rotation in the physiological set demonstrated changes in abduction from approximately 4° to the 5.3° of adduction over the whole range (Figure 2.C). More abduction in the Weak TA and more adduction in the Weak EDL with respect to the physiological load set throughout the full cycle were observed (Figure 2.D). The maximum relative differences were -2.1° and 0.9° for the Weak TA and Weak EDL at the 10° flexion. The physiological load set exhibited an increase in average Achilles load at early flexion and a decrease of the Achilles load in the rest of the cycle (Figure 2.E). Achilles load was measured for both Weak EDL and Weak TA across the entire cycle and it was lower than physiological Achilles load mainly (Figure 2.F). In comparison with the physiological load set, the Achilles load first decreased and then increased for the Weak TA while it initially increased and then decreased for the Weak EDL. Maximum load variance occurred at 20° of dorsiflexion and was 6.7 N and -21.4 N, respectively for the Weak TA and Weak EDL against the physiological load set. Significant differences were observed amongst the three sets for inversion/eversion motion (Figure 2).

DISCUSSION

According to the literature,[4] muscle weakness of the EDL or TA has an effect on the kinematics and kinetics. A change in the loading configuration within the TA and EDL muscles affects the ankle inversion and adduction at differing angles during the flexion range. In this study the ankle joint complex kinematics of both the Weak TA and the Weak EDL loading configuration deviated from the physiological one, with the largest dissimilarity observed in the inversion. The inversion amount was significant and increased during flexion for the Weak TA, which makes sense since the TA is the main invertor in the ankle. However, the Weak EDL inversion extent was not changed since the EDL is not as strong as the TA,[5] and the TA has its peak activity during the physiological loading set. The constant deviation from physiological configuration for the two loading cycle through the flexion range for AdAb can be explained by the coupling of motions between AdAb and InEv which means the various configuration make an offset in AdAb, but they change the InEv gradually. The ankles inversion and adduction behavior during plantar flexion was similar to Siegler[6] which studied the ankle three dimensional kinematics during natural motion without any loads attached to the muscles. The inversion amount in this study was considerably higher which can be understood by the attached tibialis anterior static load.

To keep the ankle stable, Achilles tendon has to resist or assist the dorsiflexion or plantarflexion motion and it is changed by the TA and EDL muscles strength. Thus, the Achilles tendon has to resist more loads to make the flexion possible when the TA load is lower at the early flexion; however, when the TA having a greater load capacity (Weak EDL), Achilles' load reduces since the resistance force is lower. The constant load difference in the mid-range of flexion was observed because of the transition state of Achilles' fibrils. Then, since the tendon is in flexion and was stabled the rest of load difference is going to increase.

The finding of this study can aid in verifying computational models, and enhance our understanding of muscle functions during flexion. There are a few limitations to this study. First the muscle loads used were relatively small compared to the physiological loads in the body. Low number of cadaveric specimen (five cadavers) was used and in order to improve the results, more specimens are needed. Tendons exhibit hysteresis while during repetitively motions; however, in this study the hysteresis effects decreased by setting up the experiment after third cycles. Moreover, variation in recognizing of the anatomical landmarks causes difference in the kinematic measurements for a single ankle; however the results for comparing between sets will not be changed.[7]

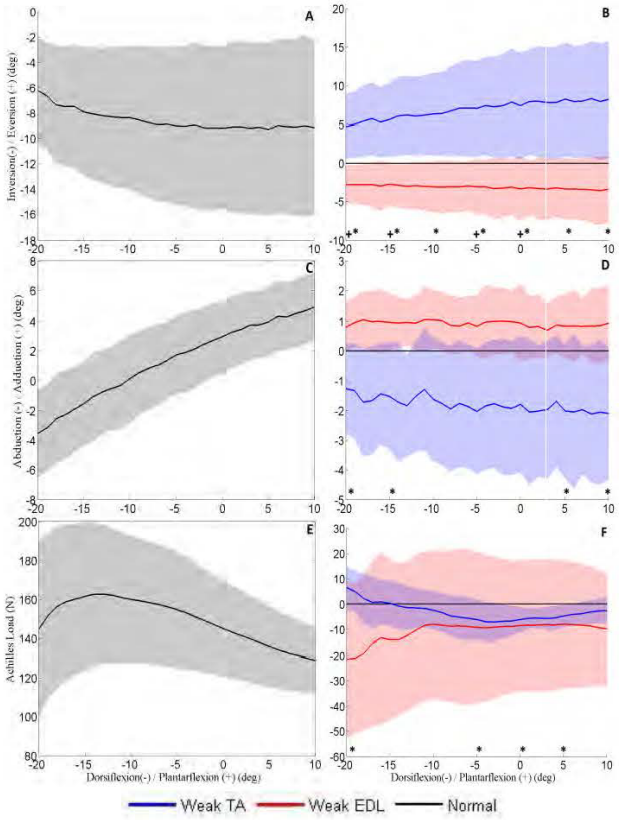

FIGURE 2: INEV (A), ADAB (C), AND LOAD (E) FOR ONE ANKLE, MEAN DIFFERENCE IN INEV (B), ADAB (D), AND LOAD (F) FOR ALL ANKLES BETWEEN PHYSIOLOGICAL AND THE OTHER TWO SETS

(SIGNIFICANCE SHOWED BY * FOR WEAK TA AND + FOR WEAK EDL)

ACKNOWLEDGEMENTS

This experiment was partially funded by DePuy Synthes, Inc.

REFERENCES

1. Payne KA, et al. J Athl Train, 32(3):221-5, 1997.
2. Slimmon D, Brukner P, 39(1-2):18-22, 2010.
3. Beckman SM, et al. Arch Phys Med Rehabil, 76(12):1138-43, 1995.
4. a hilly ller . hiladelphia aunders i 566 p. p., 1983.
5. Arnold EM, et al. Ann Biomed Eng, 38(2):269-79., 2010.
6. Siegler S, et al.. J Biomech Eng, 110(4):364-73, 1988.
7. Morton NA, et al. J of Ortho Research, 25(9):1221-1230, 2007.